
Sketchy: Memory-efficient Adaptive Regularization with Frequent Directions

Vladimir Feinberg
Google DeepMind
vladf@google.com

Xinyi Chen
Princeton University
Google DeepMind

Y. Jennifer Sun
Princeton University
Google DeepMind

Rohan Anil
Google DeepMind

Elad Hazan
Princeton University
Google DeepMind

Abstract

Adaptive regularization methods that exploit more than the diagonal entries exhibit state of the art performance for many tasks, but can be prohibitive in terms of memory and running time. We find the spectra of the Kronecker-factored gradient covariance matrix in deep learning (DL) training tasks are concentrated on a small leading eigenspace that changes throughout training, motivating a low-rank sketching approach. We describe a generic method for reducing memory and compute requirements of maintaining a matrix preconditioner using the Frequent Directions (FD) sketch. While previous approaches have explored applying FD for second-order optimization, we present a novel analysis which allows efficient interpolation between resource requirements and the degradation in regret guarantees with rank k : in the online convex optimization (OCO) setting over dimension d , we match full-matrix d^2 memory regret using only dk memory up to additive error in the bottom $d - k$ eigenvalues of the gradient covariance. Further, we show extensions of our work to Shampoo, resulting in a method competitive in quality with Shampoo and Adam, yet requiring only sub-linear memory for tracking second moments.

1 Introduction

DL optimization commonly relies on adaptive gradient methods, namely the Adam optimizer [1]. It differs from stochastic gradient descent in that the learning rate is a structured diagonal matrix built from previous gradients rather than a scalar. In full matrix AdaGrad [2], the inverse matrix square root of the sum of outer products of previous gradients is the learning rate.

Full matrix preconditioning is impractical for modern deep learning architectures: for instance, the ResNet-50 architecture [3] has over 23 million parameters, requiring more than 2 petabytes to represent its gradient covariance. Thus, diagonal preconditioning methods remain popular. However, previous work has demonstrated state-of-the-art results in some settings, such as large-batch data parallel training, for nondiagonal forms of preconditioning [4, 5, 6, 7, 8, 9]. In particular, Shampoo [5, 9] introduces a factorization of full matrix preconditioning method with adoption in large-scale industrial applications such as training Google’s ads click-through-rate model [10]. Furthermore, as hardware evolves, memory efficiency becomes an increasing concern, as “logic improves much faster than wires and SRAM, so logic is relatively free” [11]: from TPUv2 to TPUv3, per-chip `bf16` operations per second improved $2.67\times$ but memory bandwidth only improved $1.29\times$. GPUs exhibit a similar pattern for compute and memory increase, at $5\times$ and $2.2\times$, for V100 to A100 [12].

Investigation into the Kronecker-factored gradient covariance matrix reveals a concentrated, but changing, spectrum (Fig. 3), suggesting the majority of the spectral mass can be represented by a low-rank matrix, albeit rotating over time. The Frequent Directions (FD) sketch provides a mechanism to track the top eigenvectors without materializing the full covariance matrix, as proposed in [13]. Is a large portion of the spectral mass sufficient to retain the performance of adaptive regularization in theory and practice? In this work, we investigate this hypothesis.

- In the setting of online convex optimization, by applying a dynamic diagonal regularization to the FD sketch, we can **recover full-matrix AdaGrad regret up to additive spectral terms under a memory constraint**, providing a novel guarantee without curvature assumptions (Sec. 4.1). Rigorously composing our approach with Shampoo (Sec. 4.2) unlocks a **second-order algorithm which requires sub-linear memory** for its accumulators.
- By modifying FD for exponential moving averages (Sec. 4.3), we demonstrate a practical algorithm competitive with at-least-linear memory Shampoo and Adam in three modern DL settings (Sec. 5.1). While previous work [8, 14] shows rank-1 preconditioners are effective for trading off quality for memory, these results **demonstrate a Pareto improvement by using higher-rank approximations**.
- We explain the competitive performance of Sketchy with observations of fast spectral decay in the moving average of Kronecker-factored gradient covariance in DL settings (Sec. 5.2).

2 Setting and Definitions

Regret and Optimization. The optimization problem of training a deep neural network has a non-convex objective loss function f . Since finding the global optimum is computationally intractable in general, theoretical guarantees focus on convergence to an ε -approximate first-order optimum: a point x such that $\|\nabla f(x)\| \leq \varepsilon$. A smooth non-convex problem can be reduced to solving a series of offline convex problems [6]. The convex sub-problems have form $f_t(x) = f(x) + c\|x - x_t\|^2$, where c is a constant and x_t is an iterate in the optimization process. Using online-to-batch conversion, we can translate the regret bound of an online convex optimization (OCO) [15] algorithm to convergence guarantees for offline optimization. For more details of this reduction, see Appendix B.1. Therefore, non-convex optimization guarantees can be obtained from regret bounds, and we focus on the latter in this paper.

In this setting, an OCO algorithm chooses a point $x_t \in \mathcal{K}$ iteratively, where $\mathcal{K} \subseteq \mathbb{R}^d$ is a convex decision set (take $\mathcal{K} = \mathbb{R}^d$ if unconstrained). After the decision is made, the adversary reveals a convex loss function f_t , to which the algorithm suffers cost $f_t(x_t)$. Upon receiving the cost, the algorithm updates its decision for the next iteration. The regret for an online algorithm is given by

$$\text{Regret}_T = \sum_{t=1}^T f_t(x_t) - \min_{x \in \mathcal{K}} \sum_{t=1}^T f_t(x).$$

Sketching and the Frequent Directions Method. Given a stream of vectors $g_t \in \mathbb{R}^d$, $t \in [T]$, we utilize the FD sketch [13] given in Alg. 1 which maintains a low-rank approximation of the true running covariance $G_t = \sum_{s \leq t} g_s g_s^\top$. At each time t , it maintains a matrix B_t of size $d \times \ell$ whose last column is 0 and whose square is the sketch $B_t B_t^\top = \bar{G}_t$. After seeing g_t from the stream, we update the previous matrix using Alg. 1, which updates B_{t+1} of size $d \times \ell$ whose last column remains 0; take $B_0 = 0$. B_{t+1} is obtained by decomposing the sum of \bar{G}_t and the newly observed matrix, keeping only the top eigendirections, and reducing the eigenvalues uniformly by ℓ -th eigenvalue. At every iteration t , denote $\rho_t := \lambda_\ell^{(t)}$ be the removed eigenvalue from the covariance update in Alg. 1.

For convenience, let $\rho_{1:t} \stackrel{\text{def}}{=} \sum_{s=1}^t \rho_s$ be the cumulative escaped mass. For a matrix X , we denote its i -th leading eigenvalue by $\lambda_i(X)$. Let $\|\cdot\|_F$ denote the Frobenius norm of a matrix.

The fundamental property of FD is that applying Alg. 1 over a stream of vectors g_t , with $B_0 = 0$, the sum of escaped mass $\rho_t = \lambda_\ell^{(t)}$ can be bounded by the bottom eigenvalues of G_T , formally given by the following lemma:

Algorithm 1 Frequent Directions Update (FD-update)

Require: Invariant that last column of B_{t-1} is 0.

Ensure: The last column of B_t is 0.

- 1: Input: Previous state $\bar{G}_{t-1} = B_{t-1}B_{t-1}^\top \in \mathbb{R}^{d \times d}$
 - 2: Input: New symmetric PSD matrix $M_t \in \mathbb{R}^{d \times d}$.
 - 3: Eigendecompose $\bar{U}_t \text{diag } \lambda^{(t)} \bar{U}_t^\top = \bar{G}_{t-1} + M_t$ where $\lambda^{(t)}$ contains descending eigenvalues.
 - 4: Define U_t as the matrix whose columns are the first ℓ columns of \bar{U}_t , and $\lambda_{[1:\ell]}^{(t)}$ be its eigenvalues.
 - 5: Update $B_t = U_t \text{diag} \left(\lambda_{[1:\ell]}^{(t)} - \lambda_\ell^{(t)} \right)^{1/2} \cdot \lambda_\ell^{(t)}, B_t B_t^\top$.
-

Lemma 1 (Liberty [16]). *The cumulative escaped mass $\rho_{1:T}$ can be upper bounded as*

$$\rho_{1:T} \leq \min_{k=0, \dots, \ell-1} \frac{\sum_{i=k+1}^d \lambda_i(G_T)}{\ell - k} \leq \sum_{i=\ell}^d \lambda_i(G_T) \stackrel{\text{def}}{=} \lambda_{\ell:d}.$$

Proof. See Sec. B.2. □

3 Related Work

3.1 Spectral Analysis of DL Training

Denote the loss function of the i -th example for weights x as $f_i(x)$. The spectrum of the Hessian matrix $\sum_i \nabla^2 f_i$ has been the subject of intensive investigation in DL [17, 18, 19, 20] and its properties have been used to devise training methods [4, 21].

Recent papers [22, 23, 24] inspect the covariance matrix, $\sum_i (\nabla f_i)(\nabla f_i)^\top$. In small models, where its computation is feasible, these works identify fast spectral decay.

Agarwal et al. [6] take advantage of this observation by using a low-rank approximation of the whole covariance matrix, based on a limited history of the gradients, $\sum_{i=t-r}^r (\nabla f_i)(\nabla f_i)^\top$. This approach still requires r copies of the model gradients in memory, where typically r should scale with β_2^{-1} , with β_2 the exponential moving average for second order statistics (the authors set $r = 200$). Fundamentally, approximating the whole covariance matrix constrains Agarwal et al. [6] application to small models.

In our work, we validate the decay hypothesis holds across the per-layer factored covariance matrices in several modern neural networks. For a layer’s gradient matrix G_i at the i -th example and a second moment decay term β_2 , our work inspects spectral decay for $L_t = \sum_i \beta_2^{t-i} G_i G_i^\top$ and $R_t = \sum_i \beta_2^{t-i} G_i^\top G_i$; the spectral structure for these outer products is not well-documented. Furthermore, as described in Sec. 3.4, approximating the factored covariance $L_t \otimes R_t$ requires less memory than the full covariance and explains why our method can scale to large modern architectures whereas Agarwal et al. [6] cannot.

3.2 Sublinear Memory Methods

Extreme Tensoring [7], AdaFactor [14], and SM3 [8] are methods that require sublinear memory relative to the number of parameters, at the other end of the memory-quality tradeoff beyond methods that rely on the diagonal of the gradient covariance such as Adam. Owing to different structural assumptions on the set of feasible preconditioners, comparison with these methods is out of scope. However, these methods may compose with our approach. One may apply Extreme Tensoring first, then sketch the resulting reshaped tensor covariances with our method to further reduce memory consumption. Similarly, an SM3-like approach which reduces the indices for each dimension to be preconditioned can be applied before Sketchy is applied to remaining indices.

Crucially, Adam, which uses linear memory for second moment representations, compares favorably in terms of quality to all of these sublinear-memory methods. **By increasing rank in factored covariance representation, Sketchy is competitive with Adam, despite sublinear memory for**

Table 1: Memory-efficient adaptive gradient methods, in the OCO setting with dimension d (Sec. 2). We describe the worst-case regret bounds without exp-concavity assumptions, asymptotically, hiding logarithmic factors, treating the decision set diameter as a constant, and assume optimally-tuned hyperparameters. ℓ refers to the controllable preconditioner rank. Note $\text{tr} G_T^{1/2} = \sqrt{\min_{H \in \mathcal{H}} \sum_t \|\nabla_t\|_H^2}$ is the optimal preconditioner’s regret among the class of positive semi-definite, unit-trace matrices, \mathcal{H} , and G_T is the sum of gradient outer products. We let eigenvalues $\lambda_i = \lambda_i(G_T)$ with $\lambda_{i:j} = \sum_{m=i}^j \lambda_m$.

Reference	Regret (general convex)	Memory
Full Matrix AdaGrad [2]	$\text{tr} G_T^{1/2}$	d^2
Ada-LR [25]	$\text{tr} G_T^{1/2} + \lambda_{\ell+1}^{1/2} \ell^{3/4} d^{1/4}$	d^2
Ada-FD [26]	$\Omega(T^{3/4})^1$	$d\ell$
SON [27]	\sqrt{Td}	d^2
FD-SON [27]	$\sqrt{\ell \lambda_{\ell:d} T}$	$d\ell$
This paper	$\text{tr}(G_T^{1/2}) + \sqrt{d(d-\ell)\lambda_{\ell:d}}$	$d\ell$

second moment representation. Thus, for simplicity, we compare to only Adam, which dominates the alternative sublinear approaches in terms of quality.

3.3 Sketching-based Approaches

Several works have explored sketching-like approximations to the gradient covariance matrix, but none provide an adaptive bound exploiting fast spectral decay in gradient covariance without additional assumptions (Tbl. 1). In this section, we consider the OCO setting over dimension d (Sec. 2).

Random projection (Ada-LR) is most spiritually similar to our work [25]. Although it does not reduce memory usage, it relies on random projections to lower dimension $\ell \leq d$ to reduce inverse matrix computation costs. An alternative without formal guarantees, RadaGrad, reduces memory consumption to $O(d\ell)$; however, as with all Johnson-Lindenstraus projection methods, it suffers a probabilistic failure rate scaling as $O(\ell^{-1})$ (in comparison, our method inherits FD’s determinism).

Frequent Directions (FD) [13, 16], provides an alternative matrix sketching approach from the data streaming literature. As an adaptive sketch, it dominates random projection in terms of matrix recovery, and lower bounds show its memory usage is optimal in the sense that any equally-accurate approximation to an adversarially-chosen true covariance G_T in operator norm constructed from the corresponding gradients must use $O(d\ell)$ bits.

In the context of exp-concave cost functions, Luo et al. [27] provide an FD sketched version of Online Newton Step (ONS), FD-SON. In this setting, their approach nearly recovers classical ONS regret, up to logarithmic error in $\sum_{i=1}^{\ell-1} \lambda_i(G_T)$ and additive error in $\sum_{i=\ell}^d \lambda_i(G_T)$. However, without the exp-concave assumption, FD-SON falls back to a gradient-descent-like default regret of $O(\lambda_{\ell:d} \sqrt{T})$, which can be $\Omega(T)$ without spectral decay. In the context of linear bandits, Chen et al. [28] uses FD for memory reduction. The resulting algorithm, SCFD, is similar to Alg. 2, but SCFD lacks a projection step and does not handle general domains \mathcal{K} . We emphasize that our contribution is in the novelty of our regret analysis for general OCO settings, in contrast to linear bandits.

The main prior work exploring FD for general online convex settings, Wan and Zhang [26], extends the FD-SON approach by adding a fixed diagonal perturbation δI to an FD-based preconditioner, in Ada-FD. However, this approach does not achieve \sqrt{T} regret even in a non-adversarial setting with stochastic linear cost functions (Observation 2), where learning rate and δ are tuned. Dynamically changing diagonal regularization is essential for worst-case $O(\sqrt{T})$ performance.

Observation 2. Suppose we receive linear cost functions $f_t(x) = \langle x, g_t \rangle$, where $g_t \in \mathbb{R}^d$ is a random vector drawn iid from any distribution over $r \leq d$ orthonormal vectors W . For any sketch size $\ell \leq r$, the bound on the expected regret of Ada-FD is $\Omega(T^{3/4})$.

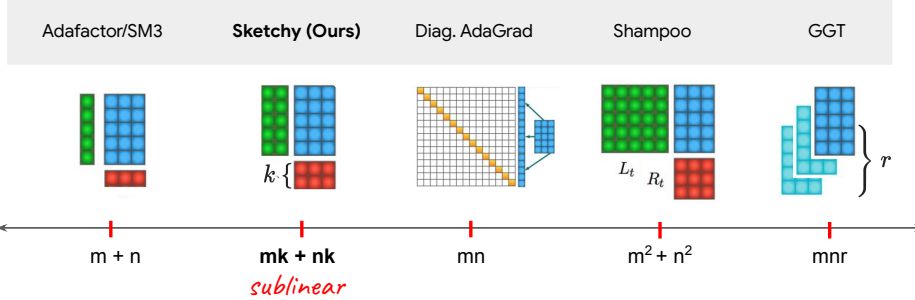


Figure 1: Asymptotic memory consumption for representing gradient covariance in adaptive regularization approaches for a single matrix parameter of size $n \times m$. Here, r refers to the GGT history buffer size and k to the approximation rank of FD (both typically set to hundreds). Past sketching approaches like Ada-FD and Radagrad take memory similar to GGT, with r being sketch size; these are all asymptotically superlinear. This figure demonstrates optimizer memory usage in the theoretical OCO setting; in practice for deep learning workloads there are additive $O(mn)$ factors for momentum, the parameters themselves, and grafting parameters for Shampoo and Sketchy.

Proof. See Sec. B.3. □

Wan and Zhang [26] remark Ada-FD has \sqrt{T} regret when G_T is low rank with rank below k , so $d - k$ of its eigenvalues are precisely zero. However, this setting does not require any sketching in the first place. By tracking the column space of observed gradients (e.g., with a reduced QR decomposition, rank-1-updated every step), the full matrix AdaGrad algorithm can be perfectly recovered without using more than $O(dk)$ memory.

In concrete convex examples, Sketchy compares favorably to these approaches (Appendix A).

3.4 Shampoo

Perhaps our most compelling application is reducing the memory of Shampoo [5, 9, 10]. Shampoo is an adaptive preconditioning method that takes into account the structure of the parameter space, and thus is more efficient than full matrix AdaGrad. For example, if the parameter is a weight matrix W of size $m \times n$, AdaGrad treats the matrix-shaped parameters as a vector of size mn , and the preconditioner has size m^2n^2 ; Shampoo instead has left and right preconditioners L, R of size $n \times n$ and $m \times m$, respectively, with the preconditioned update $L^{-1/4}WR^{-1/4}$. Write $\text{vec}(W)$ as the vectorized weights, then it is equivalent to $(L \otimes R)\text{vec}(W) = \text{vec}(LWR)$, where \otimes denotes the Kronecker product. Figure 1 illustrates the updates of AdaGrad and Shampoo, where AdaGrad update uses the entire matrix instead of the diagonal, which is shown in the figure. In other words, Shampoo uses a Kronecker-factored preconditioner, and the factorization preserves the matrix structure of the parameters. Since in DL optimization parameters often have matrix structure, Shampoo has strong empirical performance, and has improved upon state-of-the-art results in large-scale tasks such as language modeling with BERT-Large and image classification on ImageNet in [9].

Figure 1 elaborates why the composition of FD and Shampoo is essential to avoid memory consumption asymptotically greater than parameter count for approximate full matrix regularization.

However, Shampoo memory costs may still be prohibitive for rectangular weight matrices. In BERT-Large [29], most parameters are in the feed-forward network layers, which consist of 4096×1024 dense kernels; other transformers follow similar narrow-to-wide patterns. For large models, occupying even $4\times$ memory for the left preconditioner can frequently result in OOM in memory-constrained settings; this was in fact one of the practical motivations for our proposed approach.

Anil et al. [9] introduces two workarounds for the problem of rectangular matrices based on limiting covariance modelling. Furthermore, both approximations can be applied to our method, so we do not compare against them. First, the authors propose Blocked Shampoo, which views each weight matrix W of shape $m \times n$ as mn/b^2 blocks of size $b \times b$ for some block size $b < \min(m, n)$ (in the limit $b = 1$, this recovers diagonal AdaGrad). This approach is dependent on the ordering of neurons in hidden layers. Another approximation relies on only one-sided covariance upper bounds, $L_t \otimes I$ or $I \otimes R_t$. Note, however, that the one-sided approximation doesn't help with vector parameters, such as

those that appear for the bias terms in dense layers or layer norms [30]. For 3D weights, such as those which appear in homogeneous Mixtures of Experts [31], blocking increases memory consumption. These approaches do not take into account the fast decay of the preconditioner’s spectrum, which is the focus of our work.

4 Algorithms and Main Theorems

In this section, we introduce the adaptation of Frequent Directions (FD) to AdaGrad (Sec. 4.1) and Shampoo (Sec. 4.2), the corresponding algorithms and regret guarantees. Additionally, in Sec. 4.3, we modify FD to support exponential moving averages.

The main technical novelty in incorporating Alg. 1 to AdaGrad (Alg. 2) and Shampoo (Alg. 3) is the construction of preconditioning matrices with FD-sketched matrices compensated by the cumulative escaped masses. The insight of such construction lies in the observation that while the FD sketch lower bounds the full preconditioning matrix, the FD sketch compensated with the cumulative escaped masses upper bounds the full preconditioning matrix, as demonstrated in Lemma 10 for AdaGrad and Lemma 14 for Shampoo. The regret guarantee for AdaGrad ([2]) and Shampoo ([5]) directly depends on the trace of the preconditioning matrices, therefore obtaining upper and lower bounds on the preconditioning matrices allows explicit additive dependence on the cumulative escaped mass. We expect this approach to be reusable for alternative approximation schemes.

4.1 FD for AdaGrad

Our main algorithm in this section is Alg. 2 run with FD (Alg. 1) as the sketching method. $\tilde{G}_t^{-1/2}$ in Alg. 2 denotes the Moore-Penrose pseudoinverse of the matrix $\tilde{G}_t^{1/2}$. Our main algorithm, Sketchy AdaGrad, in this section exploits the FD approach outlined in Alg. 1 as the sketching method in AdaGrad. In particular, at every time step, we pass the newly received subgradient g_t into Alg. 1, which updates and maintains a low-rank sketch \tilde{G}_t of the AdaGrad preconditioning matrix G_t . We keep track of the cumulative escaped mass $\rho_{1:t}$, which we add back to the low-rank sketch to create the Sketchy preconditioner \tilde{G}_t , with which we perform the regular AdaGrad descent and projection.

Algorithm 2 Sketchy AdaGrad (S-AdaGrad)

- 1: Input: constraint set \mathcal{K} , step size η , time horizon T .
 - 2: Initialize $x_1 \in \mathcal{K}$, $\tilde{G}_0 = \tilde{G}_0 = 0$.
 - 3: **for** $t = 1, \dots, T$ **do**
 - 4: Play x_t , receive $g_t \in \partial f_t(x_t)$, suffer cost $f_t(x_t)$.
 - 5: Sketch $(\rho_t, \tilde{G}_t) = \text{FD-update}(\tilde{G}_{t-1}, g_t g_t^\top)$.
 - 6: Update $\tilde{G}_t = \tilde{G}_t + \rho_{1:t} I$, $y_{t+1} = x_t - \eta \tilde{G}_t^{-1/2} g_t$, and $x_{t+1} = \operatorname{argmin}_{x \in \mathcal{K}} \|y_{t+1} - x\|_{\tilde{G}_t^{1/2}}^2$.
 - 7: **end for**
-

Theorem 3. Define $\Omega_\ell = \min_{k < \ell} (\ell - k)^{-1} \sum_{i=k+1}^d \lambda_i(G_T)$, then with $\eta = \frac{D}{\sqrt{2}}$, Alg. 2 guarantees the following additive regret bound:

$$\text{Regret}_T(\text{S-AdaGrad}) \leq D \left(\sqrt{2} \operatorname{tr} G_T^{1/2} + d \sqrt{\frac{\Omega_\ell}{2}} \right),$$

where D is the diameter of the constraint set \mathcal{K} if \mathcal{K} is bounded and $\max_{t \in [T]} \|x_t - x^*\|_2$ otherwise.

Proof. See Sec. B.4.1. □

Notably in Thm. 3, $\text{Regret}_T = O(\sqrt{T})$ and the lower eigenvalue dependence Ω_ℓ is additive.

Corollary 4. We can improve Theorem 3 slightly to

$$\text{Regret}_T(\text{S-AdaGrad}) \leq D \left(\sqrt{2} \operatorname{tr} G_T^{1/2} + \sqrt{\frac{d(d-\ell)\Omega_\ell}{2}} \right).$$

Proof. See Sec. B.4.2. □

The regret bound above holds under the optimal tuning of the learning rate, which depends on problem quantities that can be unknown a priori. It is possible to design a parameter-free variant of Alg. 2 by using the norm $\|x\|_t = (x^\top (\tilde{G}_t + I)^{1/2} x)^{1/2}$ in the projection step of Alg. 2, as seen in [32].

4.2 FD for Shampoo

In this section, we adapt FD-update to Shampoo [5]. For simplicity, we optimize over $\mathbb{R}^{m \times n}$ in Alg. 3; projection may be handled as in Alg. 2. Similar to Sketchy AdaGrad, Sketchy Shampoo uses the FD approach outlined in Alg. 1 to sketch the left and right preconditioning matrices for Shampoo. In particular, we maintain two parallel sketching streams using Alg. 1 to produce sketches \tilde{L}_t, \tilde{R}_t for the left and right preconditioning matrices. We keep track of the cumulative escaped masses $\rho_{1:t}^L$ and $\rho_{1:t}^R$ from sketching the left and right preconditioning matrices, respectively, and compensate the cumulative escaped mass to create the left and right Sketchy preconditioning matrices \tilde{L}_t, \tilde{R}_t .

Algorithm 3 Sketchy Shampoo (S-Shampoo)

- 1: Input: step size η , time horizon T .
 - 2: Initialize $X_0 = 0_{m \times n}$, $\tilde{L}_0 = \varepsilon I_m$, $\tilde{R}_0 = \varepsilon I_n$, $\bar{L}_0 = 0_m$, $\bar{R}_0 = 0_n$.
 - 3: **for** $t = 1, \dots, T$ **do**
 - 4: Play X_t , suffer $f_t(X_t)$, receive $G_t \in \partial f_t(X_t)$.
 - 5: Sketch $(\rho_t^L, \tilde{L}_t) = \text{FD-update}(\tilde{L}_{t-1}, G_t G_t^\top)$, $(\rho_t^R, \tilde{R}_t) = \text{FD-update}(\tilde{R}_{t-1}, G_t^\top G_t)$.
 - 6: Update $\tilde{L}_t = \tilde{L}_t + \rho_{1:t}^L I_m$, $\tilde{R}_t = \tilde{R}_t + \rho_{1:t}^R I_n$ and $X_{t+1} = X_t - \eta \tilde{L}_t^{-1/4} G_t \tilde{R}_t^{-1/4}$.
 - 7: **end for**
-

Denote $L_T \stackrel{\text{def}}{=} \sum_{t=1}^T G_t G_t^\top + \varepsilon I$ and $R_T \stackrel{\text{def}}{=} \sum_{t=1}^T G_t^\top G_t + \varepsilon I$.

Theorem 5. *Suppose G_1, \dots, G_T have rank at most r . Then Alg. 3 run with $\eta = D/\sqrt{2r}$ guarantees the following regret bound:*

$$\text{Regret}_T(\mathcal{S}\text{-Shampoo}) \leq \sqrt{2r}D \left(\text{tr}(L_T^{1/4}) + m\Omega_{L,\ell}^{1/4} \right) \left(\text{tr}(R_T^{1/4}) + n\Omega_{R,\ell}^{1/4} \right),$$

where $D = \max_{t \in [T]} \|X_t - X^*\|_F$ and $\Omega_{L,\ell}, \Omega_{R,\ell}$ are analogous bounds for $\rho_{1:T}^L, \rho_{1:T}^R$ from Lem. 1.

Proof. See Sec. B.5.1. □

Bounds may be improved analogous to Cor. 4 for Alg. 3, but we omit the similar statement due to space.

4.3 Exponentially Weighted FD

This section discusses the modification of Alg. 1 to support exponential moving averages. Early in algorithm development, we noticed that attempting to approximate the unweighted sum of factored gradient covariances $\sum_t G_t G_t^\top$ and $\sum_t G_t^\top G_t$ with FD tended to an estimate of covariance that was roughly 0, creating numerical instabilities. Note that FD guarantee (Lem. 1) still holds—but the error term $\rho_{1:T}$ becomes greater than $\|G_T\|$, resulting in a vacuous bound due to lack of spectral decay.

Indeed, Fig. 3 motivating this work only confirmed that the exponential moving average $L_t(\beta_2) = \sum_t \beta_2^{T-t} G_t G_t^\top$ exhibits fast spectral decay (and analogously for R_t). Luckily, thanks to the recursion $L_{t+1}(\beta_2) = \beta_2 L_t + G_{t+1} G_{t+1}^\top$, the FD sketch may easily be adopted for this setting.

Observation 6. *Given a stream g_t of vectors for $t \in [T]$, sketch size ℓ , updates $(\rho_t^{(\beta_2)}, \bar{G}_t^{(\beta_2)}) = \text{FD-update}(\beta_2 \bar{G}_{t-1}^{(\beta_2)}, g_t g_t^\top)$, and $G_T^{(\beta_2)} = \sum_{t=1}^T \beta_2^{T-t} g_t g_t^\top$, we have*

$$\left\| \bar{G}_T^{(\beta_2)} - G_T^{(\beta_2)} \right\| \leq \rho_{1:T}^{(\beta_2)} \leq \min_{k < \ell} \frac{\sum_{i=k+1}^d \lambda_i \left(G_T^{(\beta_2)} \right)}{\ell - k}.$$

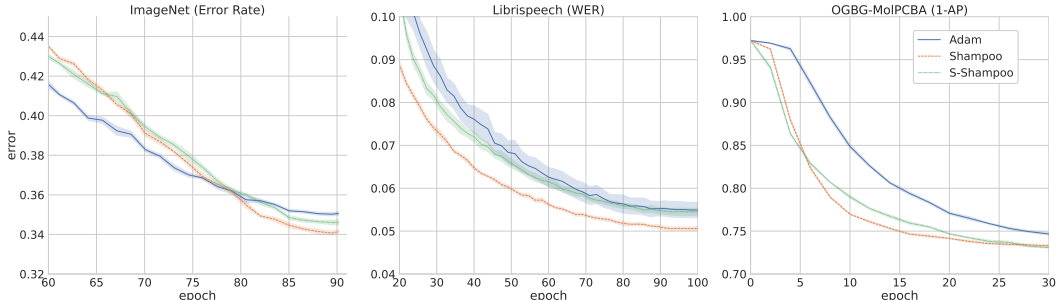


Figure 2: Test metrics are classification error rate for top-1 accuracy for ImageNet v2, word error rate for Librispeech, and one minus average precision for OGBG-MolPCBA. We plot the mean of 5 random seeds, with 1.96 times the standard error as error bars. For readers familiar with ImageNet v1, final validation accuracy for Shampoo was 77.69% (0.03%), S-Shampoo having 77.18% (0.04%), and Adam having 76.76% (0.03%), but we emphasize that due to tuning, the test set performance pictured above should be of primary concern.

5 Experiments

We investigate how much of Shampoo’s quality our low-memory approach can recover (Sec. 5.1) and whether the factored covariance exhibits spectral decay amenable to sketching (Sec. 5.2). We relegate convex examples to Appendix A due to space constraints, which check that Sketchy compares favorably to related work in a setting directly related to the theory.

5.1 Deep Neural Networks

We evaluate the effectiveness of S-Shampoo as a practical second-order algorithm for training networks, including

- ResNet-50 [3] for ImageNet image classification task of ImageNet [33] with random cropping and flipping augmentations.
- A 16-layer Conformer model [34] for the audio transcription task, Librispeech [35].
- A GNN with 5 message-passing steps [36] on ogbg-molpcba [37], which classifies structural properties of graphically encoded molecule inputs.

Our FD variant of Shampoo introduces only one new hyperparameter, the rank ℓ , which we do not tune, but set to $\ell = 256$, which translates to $4\times$ memory savings for Shampoo blocks of size 1024 for the accumulators. Shampoo, Adam, and the underlying architectures introduce their own hyperparameters. S-Shampoo inherits those of Shampoo. We tune only common parameters between the three optimizers with the same budgets, selecting based on validation set accuracy. In the ImageNet case, we evaluate final test set performance using ImageNet v2 [38], as the ImageNet test set is unavailable. Additional training information is available in Appendix C.

As Fig. 2 demonstrates, the second-order information leveraged by Shampoo results in improvements over Adam, a first-order method. Our method performs at least as well as Adam in all cases, **despite using asymptotically less memory to represent covariance** (as Fig. 1 shows, Adam uses $O(mn)$ for a rectangular weight matrix’s diagonal accumulators, whereas S-Shampoo uses $O(mk + nk)$). In the GNN case (OGBG-MolPCBA), Shampoo does not perform as well; its training curves indicate overfitting, but we note that S-Shampoo was less susceptible to overfit like Adam.

5.2 Spectral Analysis

To explain Sketchy’s strong performance in Sec. 5.1, we inspect the exponential moving average of Kronecker-factored gradient covariance for fast spectral decay. We find that this is indeed the case in practice, so Sketchy’s low-rank plus diagonal covariance is representative of true training statistics.

For all our architectures, we tune Shampoo and extract the intermediate gradient covariances over the course of training. To make our curves comparable across architectures, we fix the parameter for

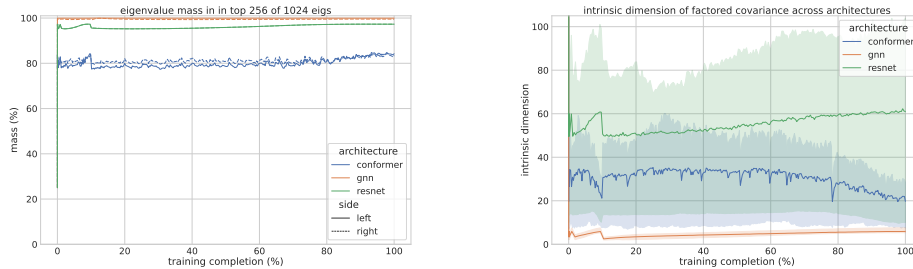


Figure 3: Two measures of spectral decay. As described in Sec. 5.2, we demonstrate spectral decay of L_t and R_t covariance factors of shape 1024×1024 . On the left, we take the factors C from the first layer of each network and plot the proportion of spectral mass captured by its top 256 eigenvalues throughout training, i.e., $\sum_{i=1}^{256} \lambda_i(C) / \sum_{i=1}^{1024} \lambda_i(C)$. On the right, we plot a continuous measure of eigenvalue concentration, the intrinsic dimension $\text{tr} C / \lambda_{\max}(C)$, typically $10\times$ smaller than nominal dimension. We plot the average across all covariances for each network’s weight’s dimensions, with the shaded regions capturing the interquartile range.

the second moment, $\beta_2 = 0.999$ for these runs. Furthermore, ResNet-50 has a few parameters with dimension 2048, but the largest dimension for any parameter from the other two architectures is 1024, so we use the Blocked Shampoo variant discussed in Sec. 3.4 with block size 1024. In other words, weights containing a dimension 2048 are split into two. We tune other Shampoo parameters for each architecture, and plot statistics of Kronecker factors $L_t = \sum_i \beta_2^{t-i} G_t G_t^\top$ and $R_t = \sum_i \beta_2^{t-i} G_t^\top G_t$.

In Fig. 3, we plot the intrinsic dimension of Kronecker covariance factors over training for our three settings. The intrinsic dimension determines the rate at which empirical covariance estimates concentrate to their expectation, rather than a random vector’s actual dimension, up to logarithmic factors (Vershynin [39], Remark 5.6.3). Despite actual dimensionality being over 1024, intrinsic dimension across all architectures stays below 105. A conspicuous phase shift 10% of the way through training may be the result of a change from linear learning rate warmup to a learning rate decay, starting at roughly 5% of the way into training.

Given $\beta_2 = 0.999$, we emphasize that the behavior in Fig. 3 is an emergent property of DL training. Though surely a lower β_2 would naturally result in lower intrinsic dimension (which can still be taken advantage of by Alg. 2 and 3), we would still expect higher intrinsic dimension if covariances were near-isometries. If we observe some large number $n = 10000$ draws x_i of $1024 \times d$ matrices with iid $N(0, 1)$ entries, then numerical experiments show that the average intrinsic dimension of $\sum_{i=0}^{n-1} \beta_2^i x_i x_i^\top$ is 324.63 (0.52) and 862.13 (0.25) for $d = 1, 64$, respectively, with parenthesized numbers denoting standard error across 20 trials. Values generated this way are larger than the average intrinsic dimension of roughly 10, 30, 50 observed in Fig. 3.

6 Discussion

Up to spectral error, Alg. 2 achieves full-matrix AdaGrad regret despite approximating the *smallest* part of the spectrum of $G_t^{-1/2}$ at each step. Remarkably, these eigenvectors correspond to the *most* easily discernible signals of the covariance for the stream g_t . This apparent (and fortuitous) coincidence is resolved by considering the covariance of $\tilde{G}_t^{-1/2} g_t$: whitening the gradient to facilitate optimization best reflects on regret; as a result, approximating top eigenvectors of G_T helps more than the bottom ones.

Our initial implementation focused on correctness rather than physical speed or memory reduction. Engineering optimizers competitive with existing industrial-strength implementations of Adam and Shampoo was out of scope. In implementing FD, we performed updates via the factored SVD of $[\beta_2^{1/2} B_t; G_t]$ rather than the eigendecomposition depicted in Alg. 1; this avoids squaring, which is unavoidable in Shampoo. For speed, Shampoo subsamples gradients for its covariance estimation and updates its inverse matrix roots intermittently, every fixed number of steps. A tuning script provided by Anil et al. [9] included gradients from every step, but updated roots every 10 steps. Since FD does

not separate sampling from its computation of estimated covariance eigendecomposition, we took the more difficult setting for S-Shampoo, only allowing it to simultaneously observe every 10th gradient and update its covariance inverse roots (see Appendix G for a theoretical justification).

Though step-skipping makes Shampoo and S-Shampoo tractable, future work may explore further speedups: since FD only requires the top ℓ eigenvalues, iterative Lanczos-like routines which are accelerator-friendly, such as LOBPCG [40], may allow incremental updates to $\tilde{G}_t^{-1/2}$ in factored form with only a few matrix multiplies, S-Shampoo may be able to update more frequently than its non-sketched counterpart, further improving quality.

7 Conclusion

In this work, we address a gap in the OCO literature for low-memory optimization with the novel Alg. 2 and demonstrate its relevance to practical non-convex problems such as neural net training (Sec. 5.1) by leveraging a new observation about gradient covariance (Sec. 5.2).

The growing disparity between compute capability and memory bandwidth [11] underscores the need for further research in this direction. Further, large-batch settings reduce the performance gap between first and Shampoo-based second order methods, since the batch-size independent runtime of the optimizer is amortized per example used for the gradient calculation. Even in performing experiments for this work, we would frequently find that faster accelerators were unavailable, but many previous-generation ones were, encouraging us to leverage data-parallel training. For datasets such as Imagenet, we notice the advantage of second order methods in dealing with large batches even at relatively modest sizes, such as 1024; many works on explore several larger multiples of this [41].

Potential for future work includes numerical methods outlined in the previous section as well optimizing the rank ℓ across the many tensors in a network, as the spread in Fig. 3 highlights the large variance in covariance intrinsic dimension. Furthermore, the inductive biases conferred by the minima which different-rank representations of curvature reach may have problem-dependent generalization implications, a question which we leave for future work. For a comparison of full rank preconditioning’s effect versus first-order minima, see Amari et al. [42].

References

- [1] Diederik P Kingma and Jimmy Ba. Adam: A method for stochastic optimization. In *ICLR (Poster)*, 2015.
- [2] John Duchi, Elad Hazan, and Yoram Singer. Adaptive subgradient methods for online learning and stochastic optimization. *Journal of machine learning research*, 12(7), 2011.
- [3] Kaiming He, Xiangyu Zhang, Shaoqing Ren, and Jian Sun. Deep residual learning for image recognition. In *Proceedings of the IEEE conference on computer vision and pattern recognition*, pages 770–778, 2016.
- [4] James Martens and Roger Grosse. Optimizing neural networks with kronecker-factored approximate curvature. In *International conference on machine learning*, pages 2408–2417. PMLR, 2015.
- [5] Vineet Gupta, Tomer Koren, and Yoram Singer. Shampoo: Preconditioned stochastic tensor optimization. In *International Conference on Machine Learning*, pages 1842–1850. PMLR, 2018.
- [6] Naman Agarwal, Brian Bullins, Xinyi Chen, Elad Hazan, Karan Singh, Cyril Zhang, and Yi Zhang. Efficient full-matrix adaptive regularization. In Kamalika Chaudhuri and Ruslan Salakhutdinov, editors, *Proceedings of the 36th International Conference on Machine Learning*, volume 97 of *Proceedings of Machine Learning Research*, pages 102–110. PMLR, 09–15 Jun 2019.
- [7] Xinyi Chen, Naman Agarwal, Elad Hazan, Cyril Zhang, and Yi Zhang. Extreme tensoring for low-memory preconditioning. In *International Conference on Learning Representations*, 2019.
- [8] Rohan Anil, Vineet Gupta, Tomer Koren, and Yoram Singer. Memory efficient adaptive optimization. *Advances in Neural Information Processing Systems*, 32, 2019.
- [9] Rohan Anil, Vineet Gupta, Tomer Koren, Kevin Regan, and Yoram Singer. Scalable second order optimization for deep learning. *arXiv preprint arXiv:2002.09018*, 2020.
- [10] Rohan Anil, Sandra Gadhanho, Da Huang, Nijith Jacob, Zhuoshu Li, Dong Lin, Todd Phillips, Cristina Pop, Kevin Regan, Gil I. Shamir, Rakesh Shivanna, and Qiqi Yan. On the factory floor: ML engineering for industrial-scale ads recommendation models, 2022.
- [11] Norman P Jouppi, Doe Hyun Yoon, Matthew Ashcraft, Mark Gottscho, Thomas B Jablin, George Kurian, James Laudon, Sheng Li, Peter Ma, Xiaoyu Ma, et al. Ten lessons from three generations shaped google’s tpuv4i: Industrial product. In *2021 ACM/IEEE 48th Annual International Symposium on Computer Architecture (ISCA)*, pages 1–14. IEEE, 2021.
- [12] William J Dally, Stephen W Keckler, and David B Kirk. Evolution of the graphics processing unit (gpu). *IEEE Micro*, 41(6):42–51, 2021.
- [13] Mina Ghashami, Edo Liberty, Jeff M Phillips, and David P Woodruff. Frequent directions: Simple and deterministic matrix sketching. *SIAM Journal on Computing*, 45(5):1762–1792, 2016.
- [14] Noam Shazeer and Mitchell Stern. Adafactor: Adaptive learning rates with sublinear memory cost. In *International Conference on Machine Learning*, pages 4596–4604. PMLR, 2018.
- [15] Elad Hazan et al. Introduction to online convex optimization. *Foundations and Trends® in Optimization*, 2(3-4):157–325, 2016.
- [16] Edo Liberty. Even simpler deterministic matrix sketching. *arXiv preprint arXiv:2202.01780*, 2022.
- [17] Levent Sagun, Leon Bottou, and Yann LeCun. Eigenvalues of the hessian in deep learning: Singularity and beyond. *arXiv preprint arXiv:1611.07476*, 2016.
- [18] Levent Sagun, Utku Evci, V Ugur Guney, Yann Dauphin, and Leon Bottou. Empirical analysis of the hessian of over-parametrized neural networks. *arXiv preprint arXiv:1706.04454*, 2017.
- [19] Behrooz Ghorbani, Shankar Krishnan, and Ying Xiao. An investigation into neural net optimization via hessian eigenvalue density. In *International Conference on Machine Learning*, pages 2232–2241. PMLR, 2019.

- [20] Adepu Ravi Sankar, Yash Khasbage, Rahul Vigneswaran, and Vineeth N Balasubramanian. A deeper look at the hessian eigenspectrum of deep neural networks and its applications to regularization. In *Proceedings of the AAAI Conference on Artificial Intelligence*, volume 35, pages 9481–9488, 2021.
- [21] Naman Agarwal, Zeyuan Allen-Zhu, Brian Bullins, Elad Hazan, and Tengyu Ma. Finding approximate local minima faster than gradient descent. In *Proceedings of the 49th Annual ACM SIGACT Symposium on Theory of Computing*, pages 1195–1199, 2017.
- [22] Guy Gur-Ari, Daniel A Roberts, and Ethan Dyer. Gradient descent happens in a tiny subspace. *arXiv preprint arXiv:1812.04754*, 2018.
- [23] Craig Bakker, Michael J Henry, and Nathan O Hodas. Understanding and exploiting the low-rank structure of deep networks. 2018.
- [24] Zeke Xie, Qian-Yuan Tang, Zheng He, Mingming Sun, and Ping Li. Rethinking the structure of stochastic gradients: Empirical and statistical evidence. *arXiv preprint arXiv:2212.02083*, 2022.
- [25] Gabriel Krummenacher, Brian McWilliams, Yannic Kilcher, Joachim M Buhmann, and Nicolai Meinshausen. Scalable adaptive stochastic optimization using random projections. *Advances in Neural Information Processing Systems*, 29, 2016.
- [26] Yuanyu Wan and Lijun Zhang. Efficient adaptive online learning via frequent directions. *IEEE Transactions on Pattern Analysis and Machine Intelligence*, 2021.
- [27] Haipeng Luo, Alekh Agarwal, Nicolo Cesa-Bianchi, and John Langford. Efficient second order online learning by sketching. *Advances in Neural Information Processing Systems*, 29, 2016.
- [28] Cheng Chen, Luo Luo, Weinan Zhang, Yong Yu, and Yijiang Lian. Efficient and robust high-dimensional linear contextual bandits. In *Proceedings of the Twenty-Ninth International Conference on International Joint Conferences on Artificial Intelligence*, pages 4259–4265, 2021.
- [29] Jacob Devlin, Ming-Wei Chang, Kenton Lee, and Kristina Toutanova. Bert: Pre-training of deep bidirectional transformers for language understanding. In *Proceedings of the 2019 Conference of the North American Chapter of the Association for Computational Linguistics: Human Language Technologies, Volume 1 (Long and Short Papers)*, pages 4171–4186, 2019.
- [30] Jimmy Lei Ba, Jamie Ryan Kiros, and Geoffrey E Hinton. Layer normalization. *arXiv preprint arXiv:1607.06450*, 2016.
- [31] Noam Shazeer, Azalia Mirhoseini, Krzysztof Maziarz, Andy Davis, Quoc Le, Geoffrey Hinton, and Jeff Dean. Outrageously large neural networks: The sparsely-gated mixture-of-experts layer. *arXiv preprint arXiv:1701.06538*, 2017.
- [32] Ashok Cutkosky. Better full-matrix regret via parameter-free online learning. In H. Larochelle, M. Ranzato, R. Hadsell, M.F. Balcan, and H. Lin, editors, *Advances in Neural Information Processing Systems*, volume 33, pages 8836–8846. Curran Associates, Inc., 2020.
- [33] Olga Russakovsky, Jia Deng, Hao Su, Jonathan Krause, Sanjeev Satheesh, Sean Ma, Zhiheng Huang, Andrej Karpathy, Aditya Khosla, Michael Bernstein, Alexander C. Berg, and Li Fei-Fei. ImageNet Large Scale Visual Recognition Challenge. *International Journal of Computer Vision (IJCV)*, 115(3):211–252, 2015. doi: 10.1007/s11263-015-0816-y.
- [34] Anmol Gulati, James Qin, Chung-Cheng Chiu, Niki Parmar, Yu Zhang, Jiahui Yu, Wei Han, Shibo Wang, Zhengdong Zhang, Yonghui Wu, et al. Conformer: Convolution-augmented transformer for speech recognition. *arXiv preprint arXiv:2005.08100*, 2020.
- [35] Vassil Panayotov, Guoguo Chen, Daniel Povey, and Sanjeev Khudanpur. Librispeech: an asr corpus based on public domain audio books. In *Acoustics, Speech and Signal Processing (ICASSP), 2015 IEEE International Conference on*, pages 5206–5210. IEEE, 2015.
- [36] Peter W Battaglia, Jessica B Hamrick, Victor Bapst, Alvaro Sanchez-Gonzalez, Vinicius Zambaldi, Mateusz Malinowski, Andrea Tacchetti, David Raposo, Adam Santoro, Ryan Faulkner, et al. Relational inductive biases, deep learning, and graph networks. *arXiv preprint arXiv:1806.01261*, 2018.
- [37] Weihua Hu, Matthias Fey, Marinka Zitnik, Yuxiao Dong, Hongyu Ren, Bowen Liu, Michele Catasta, and Jure Leskovec. Open graph benchmark: Datasets for machine learning on graphs.

- In Hugo Larochelle, Marc Aurelio Ranzato, Raia Hadsell, Maria-Florina Balcan, and Hsuan-Tien Lin, editors, *Advances in Neural Information Processing Systems 33: Annual Conference on Neural Information Processing Systems 2020, NeurIPS 2020, December 6-12, 2020, virtual*, 2020.
- [38] Benjamin Recht, Rebecca Roelofs, Ludwig Schmidt, and Vaishaal Shankar. Do imagenet classifiers generalize to imagenet? In *International Conference on Machine Learning*, pages 5389–5400, 2019.
- [39] Roman Vershynin. *High-dimensional probability: An introduction with applications in data science*, volume 47. Cambridge university press, 2018.
- [40] Andrew V Knyazev. Toward the optimal preconditioned eigensolver: Locally optimal block preconditioned conjugate gradient method. *SIAM journal on scientific computing*, 23(2):517–541, 2001.
- [41] Nitish Shirish Keskar, Dheevatsa Mudigere, Jorge Nocedal, Mikhail Smelyanskiy, and Ping Tak Peter Tang. On large-batch training for deep learning: Generalization gap and sharp minima. *arXiv preprint arXiv:1609.04836*, 2016.
- [42] Shun-ichi Amari, Jimmy Ba, Roger Baker Grosse, Xuechen Li, Atsushi Nitanda, Taiji Suzuki, Denny Wu, and Ji Xu. When does preconditioning help or hurt generalization? In *International Conference on Learning Representations*, 2020.
- [43] Luo Luo, Cheng Chen, Zhihua Zhang, Wu-Jun Li, and Tong Zhang. Robust frequent directions with application in online learning. *The Journal of Machine Learning Research*, 20(1):1697–1737, 2019.
- [44] Chih-Chung Chang and Chih-Jen Lin. Libsvm: a library for support vector machines. *ACM transactions on intelligent systems and technology (TIST)*, 2(3):1–27, 2011.
- [45] Elad Hazan, Tomer Koren, and Kfir Y Levy. Logistic regression: Tight bounds for stochastic and online optimization. In *Conference on Learning Theory*, pages 197–209. PMLR, 2014.
- [46] Adam Kalai and Santosh Vempala. Efficient algorithms for online decision problems. *Journal of Computer and System Sciences*, 71(3):291–307, 2005.
- [47] Koenraad MR Audenaert. A generalisation of mirsky’s singular value inequalities. *arXiv preprint arXiv:1410.4941*, 2014.
- [48] Justin M. Gilmer, George E. Dahl, and Zachary Nado. init2winit: a jax codebase for initialization, optimization, and tuning research, 2021. URL <http://github.com/google/init2winit>.
- [49] James Bradbury, Roy Frostig, Peter Hawkins, Matthew James Johnson, Chris Leary, Dougal Maclaurin, George Necula, Adam Paszke, Jake VanderPlas, Skye Wanderman-Milne, and Qiao Zhang. JAX: composable transformations of Python+NumPy programs, 2018.
- [50] Jonathan Heek, Anselm Levskaya, Avital Oliver, Marvin Ritter, Bertrand Rondepierre, Andreas Steiner, and Marc van Zee. Flax: A neural network library and ecosystem for JAX, 2020.
- [51] Tensorflow datasets, a collection of ready-to-use datasets. <https://www.tensorflow.org/datasets>, 2023.
- [52] Michael L. Waskom. seaborn: statistical data visualization. *Journal of Open Source Software*, 6(60):3021, 2021. doi: 10.21105/joss.03021.
- [53] J. D. Hunter. Matplotlib: A 2d graphics environment. *Computing in Science & Engineering*, 9(3):90–95, 2007. doi: 10.1109/MCSE.2007.55.
- [54] Charles R. Harris, K. Jarrod Millman, Stéfan J. van der Walt, Ralf Gommers, Pauli Virtanen, David Cournapeau, Eric Wieser, Julian Taylor, Sebastian Berg, Nathaniel J. Smith, Robert Kern, Matti Picus, Stephan Hoyer, Marten H. van Kerkwijk, Matthew Brett, Allan Haldane, Jaime Fernández del Río, Mark Wiebe, Pearu Peterson, Pierre Gérard-Marchant, Kevin Sheppard, Tyler Reddy, Warren Weckesser, Hameer Abbasi, Christoph Gohlke, and Travis E. Oliphant. Array programming with NumPy. *Nature*, 585(7825):357–362, September 2020. doi: 10.1038/s41586-020-2649-2.
- [55] Pauli Virtanen, Ralf Gommers, Travis E. Oliphant, Matt Haberland, Tyler Reddy, David Cournapeau, Evgeni Burovski, Pearu Peterson, Warren Weckesser, Jonathan Bright, Stéfan J. van der Walt, Matthew Brett, Joshua Wilson, K. Jarrod Millman, Nikolay Mayorov, Andrew R. J. Nelson, Eric Jones, Robert Kern, Eric Larson, C J Carey, İlhan Polat, Yu Feng, Eric W.

- Moore, Jake VanderPlas, Denis Laxalde, Josef Perktold, Robert Cimrman, Ian Henriksen, E. A. Quintero, Charles R. Harris, Anne M. Archibald, Antônio H. Ribeiro, Fabian Pedregosa, Paul van Mulbregt, and SciPy 1.0 Contributors. SciPy 1.0: Fundamental Algorithms for Scientific Computing in Python. *Nature Methods*, 17:261–272, 2020. doi: 10.1038/s41592-019-0686-2.
- [56] MLCommons® open engineering consortium. MLCommons Algorithmic Efficiency. <https://github.com/mlcommons/algorithmic-efficiency>, 2023.
- [57] Vijay Janapa Reddi, Christine Cheng, David Kanter, Peter Mattson, Guenther Schmuelling, Carole-Jean Wu, Brian Anderson, Maximilien Breughe, Mark Charlebois, William Chou, Ramesh Chukka, Cody Coleman, Sam Davis, Pan Deng, Greg Diamos, Jared Duke, Dave Fick, J. Scott Gardner, Itay Hubara, Sachin Idgunji, Thomas B. Jablin, Jeff Jiao, Tom St. John, Pankaj Kanwar, David Lee, Jeffery Liao, Anton Lokhmotov, Francisco Massa, Peng Meng, Paulius Micikevicius, Colin Osborne, Gennady Pekhimenko, Arun Tejusve Raghunath Rajan, Dilip Sequeira, Ashish Sirasao, Fei Sun, Hanlin Tang, Michael Thomson, Frank Wei, Ephrem Wu, Lingjie Xu, Koichi Yamada, Bing Yu, George Yuan, Aaron Zhong, Peizhao Zhang, and Yuchen Zhou. Mlperf inference benchmark, 2019.
- [58] Ilya Loshchilov and Frank Hutter. Decoupled weight decay regularization. *arXiv preprint arXiv:1711.05101*, 2017.
- [59] Boris Dayma and Rohan Anil. Evaluation of Distributed Shampoo: Comparison of optimizers: Distributed Shampoo, Adam & Adafactor. *Weights & Biases Report*, 2022.
- [60] Geoffrey Hinton, Nitish Srivastava, and Kevin Swersky. Neural networks for machine learning lecture 6a overview of mini-batch gradient descent. *Cited on*, 14(8):2, 2012.
- [61] Naman Agarwal, Rohan Anil, Elad Hazan, Tomer Koren, and Cyril Zhang. Disentangling adaptive gradient methods from learning rates. *arXiv preprint arXiv:2002.11803*, 2020.
- [62] Tsuyoshi Ando. Concavity of certain maps on positive definite matrices and applications to hadamard products. *Linear algebra and its applications*, 26:203–241, 1979.
- [63] Rajendra Bhatia. *Matrix analysis*. Springer, 1997.
- [64] Kaare Brandt Petersen, Michael Syskind Pedersen, et al. The matrix cookbook. *Technical University of Denmark*, 7(15):510, 2008.
- [65] Roger W Brockett. *Finite dimensional linear systems*. SIAM, 2015.

Table 2: Dataset statistics for simple online convex examples. We stream through each example, providing a logistic loss over the binary label and linear predictor generated by an OCO learner. The feature count includes an all-constant intercept column as well. Datasets were retrieved from Chang and Lin [44].

Dataset Name	Number of Examples	Number of Features
gisette_scale	6000	5001
a9a	32561	124
cifar10	50000	3073

Table 3: Average cumulative online loss across datasets and algorithms, ranked from lowest (1st place) to highest (6th place). Our proposal, S-Adagrad, is in bold.

	Place	1	2	3	4	5	6
cifar10	Alg.	RFD-SON	S-Adagrad	Adagrad	OGD	Ada-FD	FD-SON
	Loss	0.297	0.297	0.303	0.308	2.999	6×10^6
gisette	Alg.	S-Adagrad	RFD-SON	Ada-FD	Adagrad	OGD	FD-SON
	Loss	0.158	0.167	0.196	0.209	0.224	2.432
a9a	Alg.	Adagrad	S-Adagrad	OGD	RFD-SON	Ada-FD	FD-SON
	Loss	0.332	0.333	0.335	0.335	0.354	0.539

A Online Convex Examples

In this section, we evaluate the performance of S-Adagrad in the classical online convex optimization setting.

We consider three different datasets, summarized in Tbl. 2. For each dataset, we evaluate several works based on the frequent directions sketch, Ada-FD [26], FD-SON [27], RFD-SON [43]. As baselines we also add online gradient descent (OGD) and diagonal Adagrad [2]. For each dataset, we consider the online convex loss of a logistic binary classification loss over a linear learner on the features in each dataset augmented with a constant feature for the intercept.

For methods which require a nonzero diagonal initial regularizer δI , namely FD-SON and Ada-FD, we tune δ in $10^{-6}, 10^{-5}, \dots, 1$ and the learning rate η over the same range as well, for 49 hyperparameters total. For methods which have $\delta = 0$ (Adagrad, OGD, S-Adagrad, RFD-SON), we instead tune η on 49 points spaced evenly on the same logarithmic scale, $[10^{-6}, 1]$ to fairly allocate hyperparameter training budget. Note that the variant of RFD-SON, RFD₀, which sets $\delta = 0$ is the main variant evaluated by Luo et al. [43]. The sketch size was fixed to be 10 throughout.

We sort and display cumulative average regret in Tbl. 3 and Fig. 4. S-Adagrad is the only method to consistently place among the top three across all datasets. We suspect that a combination of allowing $\delta = 0$ (removing inductive bias about regularization; notice in Tbl. 3 that Ada-FD and FD-SON, the two methods with $\delta > 0$, routinely place last) and the ability to deal with the effectively zero exp-concavity constant of the logistic loss [45] explain S-Adagrad’s performance.

¹The regret of Ada-FD is expressed in terms of dynamic run-time quantities which do not admit a universal bound in terms of G_T ; we display its regret for the specific case of Observation 2 instead (a detailed look at its regret is given in Appendix B.3).

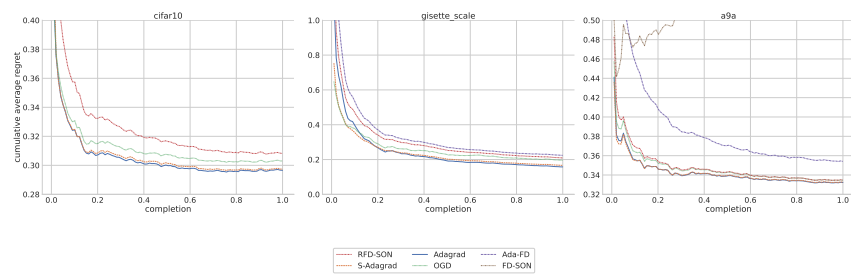


Figure 4: Cumulative average regret curves for logistic loss as a function of percent of dataset completion in a single online pass, resummarizing Tbl. 3 visually.

B Proof details

Notation. Let $\|\cdot\|$ denote the ℓ_2 norm for a vector. Let $\|\cdot\|_{op}, \|\cdot\|_F$ denote the operator norm and the Frobenius norm of a matrix, respectively. For a positive definite matrix A , we use $\|x\|_A = \sqrt{x^\top A x}$ to denote the matrix norm induced by A , and $\|x\|_A^* = \sqrt{x^\top A^{-1} x}$ to denote the dual norm of the induced matrix norm. For a matrix A , A^{-1} is the inverse of A if A is full rank; otherwise, A^{-1} is taken to be the Moore-Penrose pseudoinverse. Finally, $\overline{\text{vec}}(\cdot)$ denotes the row-major vectorization of a given matrix, and \otimes denotes the Kronecker product between two matrices

B.1 Reduction from Non-convex Optimization to Online Convex Optimization

In this section, we give more details for the reduction of non-convex optimization to online convex optimization for completeness. We use the framework of [6], though many related results exist in the optimization literature. The algorithm is stated in Algorithm 4, where we optimize the non-convex function f by iteratively optimizing subproblems f_t that are strongly convex. Given any OCO algorithm \mathcal{A} , in each episode, we first construct f_t and then use \mathcal{A} to optimize it for N time steps. We state the convergence guarantees in terms of the adaptive ratio, defined below.

Algorithm 4 Reduction from Non-convex optimization to Online Convex Optimization

- 1: Input: initial x_1 , time horizon T , episode length N , smoothness parameter L , online convex optimization algorithm \mathcal{A} .
 - 2: **for** $t = 1, \dots, T$ **do**
 - 3: Construct $f_t(x) = f(x) + L\|x - x_t\|^2$.
 - 4: Initialize \mathcal{A} to start at x_t , and set $x_t^1 = x_t$.
 - 5: **for** $n = 1, \dots, N$ **do**
 - 6: Play x_t^n , receive stochastic gradient $\tilde{\nabla}f_t(x_t^n)$, construct $g_t^n(x) = \tilde{\nabla}f_t(x_t^n)^\top(x)$.
 - 7: Update $x_t^{n+1} = \mathcal{A}(g_t^1, \dots, g_t^n)$.
 - 8: **end for**
 - 9: Update $x_{t+1} = \frac{1}{N} \sum_{n=1}^N x_t^n$.
 - 10: **end for**
 - 11: Output iterate $x_{t^*} = \operatorname{argmin}_{t \in [T+1]} \|\nabla f(x_t)\|$.
-

Definition 7. (Adaptive ratio.) Let \mathcal{A} be an algorithm, and consider a convex function f . Given a stochastic gradient oracle with variance bounded by σ^2 , let $x_{\mathcal{A}}$ be the output of \mathcal{A} with at most T oracle calls, and let $x^* \in \operatorname{argmin}_x f(x)$. Define the adaptive ratio of \mathcal{A} as

$$\mu_{\mathcal{A}}(f) = \frac{f(x_{\mathcal{A}}) - f(x^*)}{\|x_1 - x^*\| \frac{\sigma}{T}}.$$

The adaptive ratio captures the performance of \mathcal{A} relative to SGD. For certain algorithms, such as AdaGrad [2], the adaptive ratio can be as small as $\frac{1}{\sqrt{d}}$. For more discussions on this notion see [6].

Theorem 8. (Theorem A.2 in [6]) Consider a non-convex function f , and suppose f is L -smooth and bounded: $\|\nabla^2 f(x)\|_2 \leq L$ and $\max_{x,y} f(x) - f(y) \leq M$. Additionally suppose we have access to a stochastic gradient oracle with variance bounded by σ^2 . Let $\mu = \max_t \mu_{\mathcal{A}}(f_t)$. Then Algorithm 4 run with $T = \frac{12ML}{\epsilon^2}$ and $N = \frac{48\mu^2\sigma^2}{\epsilon^2}$ returns a point x_{t^*} such that

$$\mathbb{E}[\|\nabla f(x_{t^*})\|] \leq \epsilon.$$

The total number of calls to the stochastic gradient oracle is bounded by $T \cdot N = O(\mu^2 \sigma^2 / \epsilon^4)$.

B.2 Proof of Lem. 1

Proof. Let $H_T \in \mathbb{R}^{T \times d}$ denote the matrix of stacked gradients, where the t -th row of H_T is g_t . Then $H_T^\top H_T = G_T$, and FD iteratively sketches H_T . Let $H_T = U \Sigma V^\top$ be the SVD of H_T , and let $H_{T,k} = U_k \Sigma_k V_k^\top$ denote the best rank- k approximation of H_T , where U_k, V_k are the first k columns

of the matrices, and Σ_k is the upper left $k \times k$ submatrix of Σ . By the proof of Theorem 1.1 in [13], we have

$$\rho_{1:T} \leq \min_{k < \ell} \frac{\|H_T - H_{T,k}\|_F^2}{\ell - k} = \min_{k < \ell} \frac{\sum_{i=k+1}^d \lambda_i (H_T^\top H_T)}{\ell - k} = \min_{k < \ell} \frac{\sum_{i=k+1}^d \lambda_i (G_T)}{\ell - k} \leq \sum_{i=\ell}^d \lambda_i (G_T),$$

where the last inequality follows by choosing $k = \ell - 1$. \square

B.3 Proof of Observation 2

Proof. Let $\Sigma = \mathbb{E}[g_t g_t^\top]$ denote the covariance of the gradients, and $\lambda_i = \lambda_i(\Sigma)$ denote its i -th eigenvalue. By definition, g_t has the following distribution: $g_t = w_i$ with probability λ_i . At iteration t , we have the current sketch $\bar{G}_{t-1} \in \mathbb{R}^{\ell \times d}$, and we receive the new gradient g_t . Ada-FD uses $\bar{G}_{t-1} + \delta I$ as their preconditioner.

We first show that under the distribution of the cost functions, if \bar{G}_{t-1} has rank $\ell - 1$, then $\mathbb{E}[\rho_t | \bar{G}_{t-1}] \geq \sum_{i=\ell}^r \lambda_i$. Let $\bar{G}_{t-1} = U \Sigma V^\top$ be the SVD of \bar{G}_{t-1} , and v_i be the i -th row of $V \in \mathbb{R}^{\ell-1 \times d}$. Let $N_{t-1} = W \setminus \{v_1, \dots, v_{\ell-1}\}$ be the set of basis vectors not in the row space of \bar{G}_{t-1} , then $|N_{t-1}| = r - \ell + 1$. If $g_t \in \text{span}(v_1, \dots, v_{\ell-1})$, then $\rho_t = 0$; otherwise $\rho_t = 1$, with probability $\sum_{i:w_i \in N_{t-1}} \lambda_i \geq \sum_{i=\ell}^r \lambda_i$.

We proceed to bound the probability that \bar{G}_{t-1} has rank $\ell' \leq \ell - 2$. Note that this event is equivalent to having fewer than $\ell - 1$ distinct vectors drawn from W . Let I_i be the indicator variable for drawing w_i in the first $t - 1$ rounds, then we can obtain the expected number of distinct vectors as follows

$$\mathbb{E} \left[\sum_{i=1}^r I_i \right] = \sum_{i=1}^r \mathbb{E}[I_i] = \sum_{i=1}^r 1 - (1 - \lambda_i)^{t-1}.$$

We consider the random variable $r - \sum_{i=1}^r I_i$, and by Markov's inequality,

$$\mathbb{P} \left[r - \sum_{i=1}^r I_i \geq r - \ell + 2 \right] \leq \frac{\sum_{i=1}^r (1 - \lambda_i)^{t-1}}{r - \ell + 2} \leq \frac{r(1 - \lambda_r)^{t-1}}{2}.$$

Note that this is exactly the probability of having fewer than $\ell - 1$ distinct vectors in the first $t - 1$ draws. We conclude that for $t \geq \log r / \lambda_r + 1$, $\mathbb{P}[\text{rank}(\bar{G}_{t-1}) = \ell - 1] \geq \frac{1}{2}$. This implies that $\mathbb{E}[\rho_t] \geq \sum_{i=\ell}^r \lambda_i / 2$ after an initial log number of rounds, and assuming $T \geq 2 \log r / \lambda_r$,

$$\mathbb{E} \left[\sum_{t=1}^T \rho_t \right] \geq \mathbb{E} \left[\sum_{t=T/2+1}^T \rho_t \right] \geq \frac{T}{4} \sum_{i=\ell}^r \lambda_i.$$

Similarly,

$$\mathbb{E} \left[\sum_{t=1}^T \sqrt{\rho_t} \right] \geq \mathbb{E} \left[\sum_{t=T/2+1}^T \sqrt{\rho_t} \right] \geq \frac{T}{4} \sum_{i=\ell}^r \lambda_i,$$

where the second inequality holds because $\rho_t = 0$ or 1 , so $\sqrt{\rho_t} = \rho_t$ for all t . The quantities $\sum_{t=1}^T \rho_t$ and $\sum_{t=1}^T \sqrt{\rho_t}$ correspond to Δ_T and $\sum_{t=1}^T \sqrt{\sigma_t}$ in Theorem 1 of [26], respectively. Therefore, under our setting, the expectation of the upper bound in Theorem 1 is at least

$$\eta \mathbb{E} \left[\max \left\{ 1, \frac{1 + \sqrt{\sum_{t=1}^T \rho_t}}{\delta} \right\} \text{tr}(G_T^{1/2}) \right] + \frac{D^2}{2\eta} \mathbb{E} \left[\sum_{t=1}^T \sqrt{\rho_t} \right]. \quad (1)$$

If we can tune δ , then the max function evaluates to at least 1, and

$$(1) \geq \eta \mathbb{E} \left[\text{tr}(G_T^{1/2}) \right] + \frac{D^2 T}{2\eta} \sum_{i=\ell}^r \lambda_i \geq \eta \mathbb{E} \left[\sqrt{\text{tr}(G_T)} \right] + \frac{D^2 T}{8\eta} \sum_{i=\ell}^r \lambda_i = \eta \sqrt{T} + \frac{D^2 T}{8\eta} \sum_{i=\ell}^r \lambda_i,$$

where the last equality holds because $\text{tr}(G_T) = \sum_{t=1}^T \|g_t\|_2^2 = T$. Optimizing η , we conclude that the regret upper bound for Ada-FD is $\Omega(T^{3/4})$ in expectation. \square

B.4 Proof details for Section 4.1, S-AdaGrad

B.4.1 Proof of Theorem 3

The following observations are made of Algorithm 1:

Observation 9. Denote by $\bar{U}_t \stackrel{\text{def}}{=} [U_t; U_t^\perp]$. If each M_t is of rank 1, then

$$\bar{G}_t + \lambda_\ell^{(t)} I = \bar{G}_{t-1} + M_t + \lambda_\ell^{(t)} N_t ,$$

where $N_t = U_t^\perp (U_t^\perp)^\top$.

Proof. By definition of Algorithm 1, $\bar{G}_{t-1} = B_{t-1} B_{t-1}^\top$ is of rank at most $\ell - 1$. Under the assumption that M_t is of rank 1, $\bar{G}_{t-1} + M_t$ is of rank at most ℓ . Therefore, $\lambda_{\ell+1:d} = 0$. Then, we have the following:

$$\begin{aligned} \bar{G}_t + \lambda_\ell^{(t)} I &= U_t \text{diag} \left(\lambda_{[1:\ell]}^{(t)} - \lambda_\ell^{(t)} \right) U_t^\top + \lambda_\ell^{(t)} I \\ &= U_t \text{diag} \left(\lambda_{[1:\ell]}^{(t)} - \lambda_\ell^{(t)} \right) U_t^\top + \lambda_\ell^{(t)} (U_t U_t^\top + N_t) \\ &= U_t \text{diag} \lambda_{[1:\ell]}^{(t)} U_t^\top + \lambda_\ell^{(t)} N_t \\ &= \bar{U}_t \text{diag} \lambda^{(t)} \bar{U}_t^\top + \lambda_\ell^{(t)} N_t \\ &= \bar{G}_{t-1} + M_t + \lambda_\ell^{(t)} N_t . \end{aligned}$$

□

Lemma 10. Let $\lambda_\ell^{(s:t)}$ denote $\sum_{j=s}^t \lambda_\ell^{(j)}$. Let $\tilde{G}_t \stackrel{\text{def}}{=} \bar{G}_t + \lambda_\ell^{(1:t)} I$, $G_t = \sum_{s=1}^t M_s$, where each M_t is of rank 1. Let the initial $G_0 = \bar{G}_0 = 0$, then the following relation between \tilde{G}_t and G_t holds for all t :

$$\tilde{G}_t = G_t + \sum_{s=1}^t \lambda_\ell^{(s)} N_s .$$

Proof. The lemma follows from induction on t . Base case $\tilde{G}_0 = G_0$ holds by definition. Suppose the above equation holds for $t - 1$. Then,

$$\begin{aligned} \tilde{G}_t &= \bar{G}_t + \lambda_\ell^{(1:t)} I =_1 \bar{G}_{t-1} + M_t + \lambda_\ell^{(t)} N_t + \lambda_\ell^{(1:t-1)} I \\ &= \tilde{G}_{t-1} + M_t + \lambda_\ell^{(t)} N_t \\ &=_2 G_{t-1} + \sum_{s=1}^{t-1} \lambda_\ell^{(s)} N_s + M_t + \lambda_\ell^{(t)} N_t \\ &= G_t + \sum_{s=1}^t \lambda_\ell^{(s)} N_s , \end{aligned}$$

where $=_1$ follows from Observation 9 and $=_2$ follows from induction hypothesis. □

Remark 11. Note that the above lemma immediately provides an approximate isometry $\bar{G}_t \preceq G_t \preceq \tilde{G}_t$.

Now, we return to the proof of Thm. 3.

Proof. First, we make the following observation of Algorithm 2:

Observation 12. By specification of Algorithm 1,2, $g_t \in \text{span}(\tilde{G}_t)$, $\forall t$.

We follow the standard AdaGrad [2, 15] analysis. By algorithm specification,

$$\begin{aligned} y_{t+1} - x^* &= x_t - x^* - \eta \tilde{G}_t^{-1/2} g_t, \\ \tilde{G}_t^{1/2} (y_{t+1} - x^*) &= \tilde{G}_t^{1/2} (x_t - x^*) - \eta \tilde{G}_t^{1/2} \tilde{G}_t^{-1/2} g_t =_1 \tilde{G}_t^{1/2} (x_t - x^*) - \eta g_t, \end{aligned}$$

where $=_1$ follows from Observation 12.

With standard AdaGrad analysis, we can bound regret Regret_T above by the sum of the diameter bound and the gradient bound:

$$\underbrace{\frac{1}{2\eta} \sum_{t=1}^T \|x_t - x^*\|_{\tilde{G}_t^{1/2} - \tilde{G}_{t-1}^{1/2}}^2}_{R_D} + \underbrace{\frac{\eta}{2} \sum_{t=1}^T \|g_t\|_{F_t^{-1/2}}}_{R_G}.$$

Note that by algorithm specification, we have $\forall t$,

$$\tilde{G}_t = \bar{G}_t + \rho_{1:T} I =_1 \tilde{G}_{t-1} + g_t g_t^\top + \rho_t N_t \succeq \tilde{G}_{t-1} + g_t g_t^\top,$$

where $=_1$ follows from the proof of Lemma 10. In particular, $\tilde{G}_t \succeq \tilde{G}_{t-1}$.

Using Remark 11, the gradient norm term in the regret bound can be further bounded by

$$R_G = \frac{\eta}{2} \sum_{t=1}^T g_t^\top \tilde{G}_t^{-1/2} g_t \leq \frac{\eta}{2} \sum_{t=1}^T g_t^\top G_t^{-1/2} g_t \leq \eta \text{tr} \left(G_T^{1/2} \right),$$

where the last inequality follows from Lemma 10 of Duchi et al. [2].² The diameter norm term in the regret bound can be bounded by

$$\begin{aligned} R_D &= \frac{1}{2\eta} \sum_{t=1}^T \|x_t - x^*\|_{\tilde{G}_t^{1/2} - \tilde{G}_{t-1}^{1/2}}^2 \leq_1 \frac{D^2}{2\eta} \text{tr} \left(\tilde{G}_T^{1/2} \right) \\ &\leq \frac{D^2}{2\eta} \text{tr} \left((G_T + \rho_{1:T} I)^{1/2} \right) \\ &\leq_2 \frac{D^2}{2\eta} \left(\text{tr} G_T^{1/2} + \text{tr}(\rho_{1:T} I)^{1/2} \right), \end{aligned}$$

where \leq_1 follows from monotonicity of \tilde{G}_t 's, $\|\cdot\|_{op} \leq \text{tr}(\cdot)$ for positive semidefinite matrices, and linearity of $\text{tr}(\cdot)$, and \leq_2 follows from that for $X \in \mathbb{R}^d$, $X \succeq 0$, $\text{tr}(X + \sigma I_d)^{1/2} \leq \text{tr}(X^{1/2}) + d\sqrt{\sigma}$. Combining, we have

$$\text{Regret}_T \leq \frac{d\sqrt{\rho_{1:T}} + \text{tr} G_T^{1/2}}{2\eta} D^2 + \eta \text{tr} \left(G_T^{1/2} \right) = D \left(\sqrt{2} \text{tr} G_T^{1/2} + d\sqrt{\frac{\rho_{1:T}}{2}} \right),$$

where the last equality is established by choosing $\eta = \frac{D}{\sqrt{2}}$. \square

B.4.2 Proof of Corollary 4

Proof. Following the proof of Theorem 3, we have

$$\text{Regret}_T \leq \frac{D^2 \text{tr} \tilde{G}_t^{1/2}}{2\eta} + \eta \text{tr} G_T^{1/2},$$

Denote the accumulated error term

$$E = \sum_{t=1}^T \rho_t N_t.$$

²The FTL-BTL lemma [46] alone is not sufficient to justify this inequality, at least interpreting $G^{-1/2}$ as $(G^{1/2})^+$. However, Duchi et al. [2] rely on concavity of $X \mapsto \text{tr} X^{1/2}$ to show a semidefinite version of the statement.

Then, by Lemma 10 and sub-additivity of $\text{tr} \left((\cdot)^{1/2} \right)$ [47],

$$\text{Regret}_T \leq \left(\frac{D^2}{2\eta} + \eta \right) \text{tr} G_T^{1/2} + \frac{D^2}{2\eta} \text{tr} E^{1/2},$$

where it remains to bound the last term. Let Q be a matrix with column vectors q_i that forms an eigenbasis of $E^{1/2}$; this diagonalizes E as well. Notice that

$$\lambda_i(E) = \sum_{t=1}^T \rho_t q_i^\top N_t q_i,$$

and since

$$\lambda_i^{1/2}(E) = \lambda_i(E^{1/2}),$$

that we can characterize

$$\text{tr} E^{1/2} = \sum_{i=1}^d \lambda_i^{1/2}(E) = \sum_{i=1}^d \left(\sum_{t=1}^T \rho_t q_i^\top N_t q_i \right)^{1/2}.$$

Denote $u_{t,i} = q_i^\top N_t q_i$, since N_t is a rank- $(d - \ell)$ projection, $\|u_t\|_1 = d - \ell$. Then $\text{tr} E^{1/2}$ is upper bounded by the value of the program

$$\begin{aligned} \max_{u_{t,i}} \quad & \sum_{i=1}^d \left(\sum_{t=1}^T \rho_t u_{t,i} \right)^{1/2} \\ \text{s.t.} \quad & \sum_{i=1}^d u_{t,i} = d - \ell \quad \forall t \in [T]. \end{aligned}$$

Note that

$$\sum_{i=1}^d \left(\sum_{t=1}^T \rho_t u_{t,i} \right)^{1/2} \leq_1 \sqrt{d} \sqrt{\sum_{i=1}^d \sum_{t=1}^T \rho_t u_{t,i}} = \sqrt{d} \sqrt{\sum_{t=1}^T \rho_t \sum_{i=1}^d u_{t,i}} =_2 \sqrt{d \rho_{1:T} (d - \ell)},$$

where \leq_1 follows from Cauchy-Schwarz, and $=_2$ follows from the constraint on $\sum_{i=1}^d u_{t,i}$.

Combining, we have

$$\text{Regret}_T \leq \frac{\sqrt{d(d - \ell) \rho_{1:T}} + \text{tr} G_T^{1/2}}{2\eta} D^2 + \eta \text{tr} G_T^{1/2} = D \left(\sqrt{2} \text{tr} G_T^{1/2} + \sqrt{\frac{d(d - \ell) \rho_{1:T}}{2}} \right),$$

where the last equality follows from the choice of step size $\eta = \frac{D}{\sqrt{2}}$. □

B.5 Proof details for Section 4.2, S-Shampoo

B.5.1 Proof of Theorem 5

Proof. First, we establish the following observation and lemma analogous to Observation 9 and Lemma 10:

Observation 13 (Analogous to Observation 9). *Let $V_t \Sigma_t^L V_t^\top = \bar{L}_{t-1} + G_t G_t^\top$ be the eigen-decomposition of the un-deflated sketch, where $V_t \in \mathbb{R}^{m \times m}$. Suppose $\text{rank}(\Sigma_t^L) = k$, where $k \in [\ell - 1, \ell - 1 + r]$. Write $V_t = [V_t^\parallel V_t^\perp]$, where V_t^\parallel contain the first k columns of V_t . Then by definition*

$$\bar{L}_t + \rho_t^L I \succeq \bar{L}_{t-1} + G_t G_t^\top + \rho_t^L V_t^\perp (V_t^\perp)^\top.$$

Analogously for the right conditioner, let $W_t \Sigma_t^R W_t^\top = \bar{R}_{t-1} + G_t^\top G_t$, and write $W_t = [W_t^\parallel W_t^\perp]$, then

$$\bar{R}_t + \rho_t^R I \succeq \bar{R}_{t-1} + G_t^\top G_t + \rho_t^R W_t^\perp (W_t^\perp)^\top.$$

Lemma 14. (Analogous to Lemma 10) Define $N_t^L = V_t^\perp (V_t^\perp)^\top$, $N_t^R = W_t^\perp (W_t^\perp)^\top$, then

$$\tilde{L}_t \succeq \sum_{s=1}^t G_s G_s^\top + \sum_{s=1}^t \rho_s^L N_s^L + \varepsilon I_m, \quad \tilde{R}_t \succeq \sum_{s=1}^t G_s^\top G_s + \sum_{s=1}^t \rho_s^R N_s^R + \varepsilon I_n.$$

We follow the shampoo proof in [5]. Let $x_t = \overline{\text{vec}}(X_t)$, $g_t = \overline{\text{vec}}(G_t)$, where $\overline{\text{vec}}(\cdot)$ denote the row-major vectorization of a given matrix.

Kronecker product \otimes obeys the following properties as shown in [5]:

Lemma 15 (Lemma 3,4 in Gupta et al. [5]). *For matrices A, A', B, B' of appropriate dimensions and vectors $u, v, L \in \mathbb{R}^{m \times m}, R \in \mathbb{R}^{n \times n}, G \in \mathbb{R}^{m \times n}$, the following properties hold:*

1. $(A \otimes B)(A' \otimes B') = (AA') \otimes (BB')$.
2. $(A \otimes B)^\top = A^\top \otimes B^\top$.
3. $A, B \succeq 0, (A \otimes B)^{-1} = A^{-1} \otimes B^{-1}$.
4. $A \succeq A', B \succeq B'$, then $A \otimes B \succeq A' \otimes B'$.
5. $\text{tr}(A \otimes B) = \text{tr}(A) + \text{tr}(B)$.
6. $\overline{\text{vec}}(uv^\top) = u \otimes v$.
7. $(L \otimes R^\top) \overline{\text{vec}}(G) = \overline{\text{vec}}(LGR)$.

Then the shampoo update is

$$x_{t+1} = x_t - \eta(\tilde{L}_t^{1/4} \otimes \tilde{R}_t^{1/4})^{-1} g_t.$$

Let $\tilde{H}_t \stackrel{\text{def}}{=} \tilde{L}_t^{1/4} \otimes \tilde{R}_t^{1/4}$, then by Lemma 15, \tilde{H}_t is monotone increasing with t , since \tilde{L}_t and \tilde{R}_t are monotone by Observation 13. Thus, by standard analysis [15] for Online Mirror Descent (OMD), we can break down the regret into the diameter bound and the gradient bound:

$$\text{Regret}_T \leq R_D + R_G, \quad \text{where}$$

f

$$R_D = \frac{1}{2\eta} \sum_{t=1}^T \left(\|x_t - x^*\|_{\tilde{H}_t}^2 - \|x_{t+1} - x^*\|_{\tilde{H}_t}^2 \right), \quad R_G = \frac{\eta}{2} \sum_{t=1}^T \left(\|g_t\|_{\tilde{H}_t}^* \right)^2.$$

We proceed to bound R_D and R_G separately. For R_D ,

$$\begin{aligned} R_D &\leq \frac{1}{2\eta} \sum_{t=1}^T \|x_t - x^*\|_{\tilde{H}_t - \tilde{H}_{t-1}}^2 + \|x_1 - x^*\|_{\tilde{H}_0}^2 \\ &\leq \frac{1}{2\eta} \sum_{t=1}^T \|\tilde{H}_t - \tilde{H}_{t-1}\|_{op} \|x_t - x^*\|_2^2 + \|x_1 - x^*\|_{\tilde{H}_0}^2 \\ &\leq_1 \frac{D^2}{2\eta} \sum_{t=1}^T \text{tr}(\tilde{H}_t - \tilde{H}_{t-1}) + \|x_1 - x^*\|_{\tilde{H}_0}^2 \\ &\leq \frac{D^2}{2\eta} \text{tr}(\tilde{H}_T), \end{aligned}$$

where \leq_1 holds since \tilde{H}_t 's are increasing in t , and we have for positive semidefinite matrices $\text{tr}(\cdot) \geq \|\cdot\|_{op}$.

Now we try to bound R_G . First, we have that

Lemma 16 (Lemma 8 in Gupta et al. [5]). *If $G \in \mathbb{R}^{m \times n}$ with rank at most r , and $g = \overline{\text{vec}}(G)$, then $\forall \varepsilon \geq 0, \forall t$,*

$$\varepsilon I_{mn} + \frac{1}{r} \sum_{s=1}^t g_s g_s^\top \preceq \left(\varepsilon I_m + \sum_{s=1}^t G_s G_s^\top \right)^{1/2} \otimes \left(\varepsilon I_n + \sum_{s=1}^t G_s^\top G_s \right)^{1/2}.$$

Define $M_t^L \in \mathbb{R}^{m \times m}, M_t^R \in \mathbb{R}^{n \times n}$ by

$$M_t^L \stackrel{\text{def}}{=} \sum_{s=1}^t G_s G_s^\top + \sum_{s=1}^t \rho_s^L N_s^L + \varepsilon I_m, \quad M_t^R \stackrel{\text{def}}{=} \sum_{s=1}^t G_s^\top G_s + \sum_{s=1}^t \rho_s^R N_s^R + \varepsilon I_n,$$

then by Lemma 14,

$$\tilde{L}_t \succeq M_t^L, \quad \tilde{R}_t \succeq M_t^R.$$

Observe that in addition,

$$M_t^L \succeq \varepsilon I_m + \sum_{s=1}^t G_s G_s^\top, \quad M_t^R \succeq \varepsilon I_n + \sum_{s=1}^t G_s^\top G_s.$$

Again by Lemma 15,

$$I_m \otimes \left(\varepsilon I_n + \sum_{s=1}^t G_s^\top G_s \right) \preceq I_m \otimes M_t^R, \quad \left(\varepsilon I_m + \sum_{s=1}^t G_s G_s^\top \right) \otimes I_n \preceq M_t^L \otimes I_n.$$

Combining, we have

$$\varepsilon I_{mn} + \frac{1}{r} \sum_{s=1}^t g_s g_s^\top \preceq (M_t^L)^{1/2} \otimes (M_t^R)^{1/2} \preceq \tilde{L}_t^{1/2} \otimes \tilde{R}_t^{1/2}.$$

Define $\hat{H}_t \succ 0 \forall t \in [T]$ by

$$\hat{H}_t \stackrel{\text{def}}{=} \left(r \varepsilon I_{mn} + \sum_{s=1}^t g_s g_s^\top \right)^{1/2} \preceq \sqrt{r} \tilde{H}_t.$$

The bound on R_G depends on the following lemma:

Lemma 17 (Lemma 2 in Gupta et al. [5]). *Consider a sequence of vectors $\{g_t\}_{t=1}^T$. Given a function $\Phi(\cdot)$ over positive semidefinite matrices,*

$$\sum_{t=1}^T (\|g_t\|_{H_t}^*)^2 \leq \sum_{t=1}^T (\|g_t\|_{H_T}^*)^2 + \Phi(H_T) - \Phi(H_0),$$

where

$$H_t = \underset{H \succ 0}{\text{argmin}} \left\{ \left(\sum_{s=1}^t g_s g_s^\top \right) \cdot H^{-1} + \Phi(H) \right\}.$$

Let $\Phi(H) \stackrel{\text{def}}{=} \text{tr}(H) + r \varepsilon \text{tr}(H^{-1})$ and since

$$\underset{H \succ 0}{\text{argmin}} \left\{ \left(\sum_{s=1}^t g_s g_s^\top \right) \cdot H^{-1} + \Phi(H) \right\} = \underset{H \succ 0}{\text{argmin}} \left\{ \text{tr}(\hat{H}_t^2 H^{-1} + H) \right\} = \hat{H}_t,$$

the above lemma gives

$$\sum_{t=1}^T (\|g_t\|_{\hat{H}_t}^*)^2 \leq \sum_{t=1}^T (\|g_t\|_{\hat{H}_T}^*)^2 + \Phi(\hat{H}_T) - \Phi(\hat{H}_0) \leq 2 \text{tr}(\hat{H}_T),$$

which by inequality of \hat{H}_t and \tilde{H}_t established above, gives

$$R_G \stackrel{\text{def}}{=} \frac{\eta}{2} \sum_{t=1}^T \left(\|g_t\|_{\hat{H}_t}^* \right)^2 \leq \frac{\eta\sqrt{r}}{2} \sum_{t=1}^T \left(\|g_t\|_{\tilde{H}_t}^* \right)^2 \leq \eta\sqrt{r} \operatorname{tr}(\hat{H}_T) \leq \eta r \operatorname{tr}(\tilde{H}_T).$$

Combining the bound on R_D and R_G , the overall regret is

$$\operatorname{Regret}_T \leq R_D + R_G \leq \left(\frac{D^2}{2\eta} + \eta r \right) \operatorname{tr}(\tilde{H}_T) = \sqrt{2r} D \operatorname{tr}(\tilde{H}_T) = \sqrt{2r} D \operatorname{tr}(\tilde{L}_T^{1/4}) \operatorname{tr}(\tilde{R}_T^{1/4}).$$

by the choice of $\eta = \frac{D}{\sqrt{2r}}$ and trace multiplicative equality in Lemma 15. Finally, we have

$$\begin{aligned} \operatorname{tr}(\tilde{L}_T^{1/4}) &\leq_1 \operatorname{tr}(\bar{L}_T^{1/4}) + \operatorname{tr}\left((\rho_{1:T}^L I_m)^{1/4}\right) \\ &\leq_2 \operatorname{tr}\left(\left(\sum_{t=1}^T G_t G_t^\top + \varepsilon I\right)^{1/4}\right) + m (\rho_{1:T}^L)^{1/4} \\ &= \operatorname{tr}(L_T^{1/4}) + m (\rho_{1:T}^L)^{1/4}, \end{aligned}$$

where \leq_1 follows from definition of \tilde{L}_T in Algorithm 3 and subadditivity of $\operatorname{tr}((\cdot)^{1/4})$ [47], \leq_2 follows from Remark 11. Similarly,

$$\operatorname{tr}(\tilde{R}_T^{1/4}) \leq \operatorname{tr}(R_T^{1/4}) + n (\rho_{1:T}^R)^{1/4}.$$

□

B.5.2 Proof of Lemma 14

Proof. We will show the first inequality as the second inequality holds analogously. For $t = 0$, $\tilde{L}_0 = \varepsilon I_m$ by definition of algorithm. Suppose the first inequality holds for t . Consider $t + 1$:

$$\begin{aligned} \tilde{L}_{t+1} &= \bar{L}_{t+1} + \rho_{1:t+1}^L I_m \\ &\succeq_1 \bar{L}_t + G_{t+1} G_{t+1}^\top + \rho_{t+1}^L N_{t+1} + \rho_{1:t}^L I_m \\ &= \tilde{L}_t + G_{t+1} G_{t+1}^\top + \rho_{t+1}^L N_{t+1} \\ &\succeq_2 \sum_{s=1}^{t+1} G_s G_s^\top + \sum_{s=1}^{t+1} \rho_s^L N_s^L + \varepsilon I_m, \end{aligned}$$

where \succeq_1 follows from Observation 13 and \succeq_2 follows from induction hypothesis. □

Table 4: The search space for hyperparameters for tuning Shampoo on our NN architectures for the Kronecker-factored covariance optimization. Note that the search space explores one less momentum, not momentum directly. Label smoothing was only applied to ImageNet. We sample uniformly either from linear or logscale among the ranges specified with 100 trials, and select the best one according to validation accuracy.

Hyperparameter	Range	Log scale?
Learning rate η	$[10^{-4}, 10^{-2}]$	✓
Weight decay γ	$[10^{-2}, 1]$	✓
Momentum $1 - \beta_1$	$[10^{-2}, 10^{-1}]$	✓
Label smoothing	$[0, 0.2]$	

C Training Settings

For repeatable, standard evaluation on modern, competitive tasks we use `init2winit` [48] for Jax [49] implementations of architectures in Flax [50] and standard dataset preprocessing built on top of TFDS [51]. We rely on standard scientific packages for conducting our work [52, 53, 54, 55]. Our source code will be released after publication.

Neural net architecture settings are taken from the default settings of the `init2winit` library at hash `e337ffe` [48], which reference the MLCommons specifications provided at MLCommons® open engineering consortium [56], including the MLPerf ResNet-50 variant [57], Conformer, and GNN. The Distributed Shampoo implementation was run at hash `83e6e62` in the repository referenced by Anil et al. [9].

Throughout, weight decay is applied using its decoupled variant [58].

We requested a Shampoo tuning script from Dayma and Anil [59], Anil et al. [9], which fixed several parameters for Shampoo outside the usual defaults. We tuned on a cluster of TPUv4s, with 16 TPUv4s per trial in data-parallel mode.

- Block size was already set to 1024. As mentioned in Sec. 5.2, we kept this change for consistency in covariance factor size across architectures.
- Preconditioning was set to start 101 steps into training (`start_preconditioning_step`).
- Preconditioners were updated every 10 steps instead of every step for speed (`preconditioning_compute_steps` is 10).
- The grafting type, which controls the per-tensor learning rate schedule, was set to `RMSPROP_NORMALIZED`, which applies RMSProp [60] over unit-normalized gradients.
- `moving_average_for_momentum` was activated (so the final updates are computed as $\beta_1\mu_t + (1 - \beta_1)g_t$, where μ_t is the momentum term and g_t is the preconditioned update).
- The virtual batch size, used to compute batch norm statistics, was set to 32 (the full per-step minibatch size was 1024, but this enables data-parallel training).

Also from the provided script, we used a linear warmup rampup starting from 0 to the nominal learning rate hyperparameter setting, followed by a cosine decay schedule, with the transition happening 5% of the way into training (the learning rate monotonically increases, then monotonically decreases, as the cosine schedule has a quarter-period set to the number of training steps).

Then, we performed tuning using random hyperparameter search over the space defined in Tbl. 4. We ran the batch sizes and number of steps provided in the scripts, which were 256, 512, 1024 for Conformer, GNN, and ResNet-50, respectively, for about 162, 117, 199 epochs, respectively.

Shampoo is automatically configured with grafting parameters, which we search over [61].

D ResNet-50 Settings

For training ImageNet, we mostly inherited the settings of Appendix C for Shampoo tuning, but made some minor modifications, namely adding of the second moment decay (β_2), widening the search

Table 5: The search space for hyperparameters for tuning Shampoo on our architectures for ImageNet hyperparameters. The same space was applied to S-Shampoo with a fixed sketch rank $\ell = 256$ for all tensors. Note that we search $1 - \beta_1, 1 - \beta_2$, and not the original hyperparameter. We sample uniformly either from linear or logscale among the ranges specified with 256 trials, and select the best one according to validation accuracy. (*) stands for a discrete uniform choice over four different grafting rates, based on AdaGrad, RMSProp, and normalized versions of the two. The gradient clipping norm is similarly discrete.

Hyperparameter	Range	Log?
Learning rate η	$[10^{-4}, 10^{-2}]$	✓
Weight decay γ	$[10^{-3}, 0.1]$	✓
Momentum $1 - \beta_1$	$[10^{-4}, 10^{-1}]$	✓
2 nd moment $1 - \beta_2$	$[10^{-4}, 10^{-1}]$	✓
Label smoothing	$[0, 0.2]$	
Dropout Rate	$[0, 0.2]$	
Grafting Type	(*)	
Gradient Clip L_2	$\{1, 10, 10^2, 10^3\}$	

Table 6: The search space for hyperparameters for tuning Adam on our architectures for ImageNet hyperparameters. The same caveats as in Tbl. 5 apply. Also tuned with 256 trials.

Hyperparameter	Range	Log?
Learning rate η	$[10^{-4}, 10^{-2}]$	✓
Weight decay γ	$[10^{-3}, 0.1]$	✓
Momentum $1 - \beta_1$	$[10^{-4}, 10^{-1}]$	✓
2 nd moment $1 - \beta_2$	$[10^{-4}, 10^{-1}]$	✓
Label smoothing	$[0, 0.2]$	
Dropout Rate	$[0, 0.2]$	
Warmup Duration	$[2\%, 10\%]$ of training	
Gradient Clip L_2	$\{1, 10, 10^2, 10^3\}$	

space, and, for computational reasons, performing a shortened run of only 66 epochs for tuning trials. The architecture details remain the same. The learning rate schedule was stretched to this interval, so warmup was still 5% of the duration, and cosine decay ended learning rate at 0 by the end of the 66 epochs of training. The full search space is elaborated on in Tbl. 5.

To tune Adam, a first order method, we considered mostly the same nominally hyperparameters (where β_2 refers to second moment momentum now), except grafting, which instead we replaced with a search over the warmup duration, summarized in Tbl. 6.

Full evaluation of the selected best hyperparameters for each setting was performed with the classical 90-epoch setting, with the learning rate schedule correspondingly stretched.

We provide the full training curves in Fig. 5.

E Conformer Settings

The Conformer architecture was used from the MLCcommons specification as described in Appendix C, with the following fixed additional settings: 1024 batch size, 100 epochs of training, 5% of training used for linear warmup with cosine decay of learning rate. We fixed gradient clipping at a value of 10, without which we noticed Adam curves were very volatile. We set the `eight` parameter for Shampoo to true (we found that it did not make a difference in a few sample runs' loss curves, as an alternative to the iterative p -th inverse root routine in Shampoo, but used it instead since we believe it has better numerical stability). The hyperparameters we searched over for all optimizers are described in Tbl. 7.

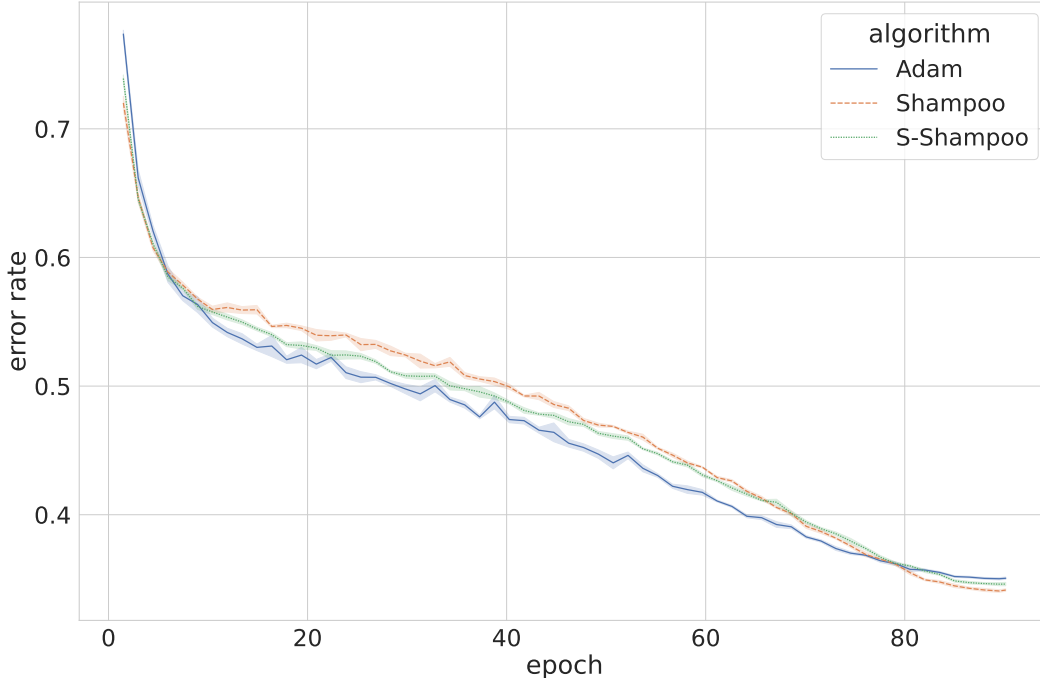


Figure 5: Full test set curves for imagenet.

Table 7: The search space for hyperparameters for tuning Shampoo, Adam, and S-Shampoo for Conformer with fixed 256 rank. Here we fixed the grafting type to be RMSProp. During initial runs of the baselines, we noticed that Adam preferred larger learning rates, so we changed and reran its space for η to be $10\times$ that of Shampoo, namely $[10^{-4}, 10^{-2}]$, still searching over logspace. We also stopped any hyperparameter trial which did not go below 0.875 WER after 5000 training steps.

Hyperparameter	Range	Log?
Learning rate η	$[10^{-5}, 10^{-3}]$	✓
Momentum $1 - \beta_1$	$[10^{-3}, 10^{-1}]$	✓
2 nd moment $1 - \beta_2$	$[10^{-3}, 10^{-1}]$	✓
Weight decay γ	$[10^{-4}, 10^{-2}]$	✓
Dropout Rate	$[0, 0.2]$	✓

F GNN Settings

The GNN architecture was used from the MLCommons specification as described in Appendix C, with the following fixed additional settings: 1024 batch size, 30 epochs of training, 5% of training used for linear warmup with cosine decay of learning rate, 0.05 dropout, and we set the `epoch` parameter for Shampoo to true as in Appendix E.

Then we searched a hyperparameter space for Shampoo, Adam, and S-Shampoo as described in Tbl. 8.

Table 8: The search space for hyperparameters for tuning Shampoo and S-Shampoo for GNN with fixed regularization settings (due to resource constraints, we only ran 128 samples from the grid here). Here we fixed the grafting type to be RMSProp and did not use gradient clipping, unlike Tbl. 5, based on a few trial runs of the Shampoo baseline from which we determined we could reduce the hyperparameter space.

Hyperparameter	Range	Log?
Learning rate η	$[10^{-4}, 10^{-2}]$	✓
Momentum 1 $-\beta_1$	$[10^{-3}, 0.5]$	✓
2 nd moment 1 $-\beta_2$	$[10^{-3}, 0.5]$	✓
Weight decay γ	$[10^{-3}, 0.5]$	✓

G Step-skipping

In this section, we provide some theoretical justification for step-skipping. We first derive the regret bound of AdaGrad with step skipping, named Generic Epoch AdaGrad. The additional regret incurred is expressed as an error term. Then, we describe a setting where the error term admits a simple bound, showing that step-skipping incurs at most an extra $\log T$ time dependence on the regret.

G.1 Adversarial losses

Consider a generalized epoching AdaGrad with K fixed update points t_k , such that $t_1 = 0$ and $t_K = T$.

Algorithm 5 Generic Epoch AdaGrad

- 1: Input: $\eta, T, \{t_k\}_{k=1}^K, G_0 \succ 0$, convex closed set \mathcal{K} .
 - 2: Initialize: x_1 .
 - 3: **for** $k = 1, \dots, K - 1$ **do**
 - 4: **for** $t = t_k + 1, \dots, t_{k+1}$ **do**
 - 5: Play x_t , receive f_t loss with gradient g_t .
 - 6: Update $G_t = G_{t-1} + g_t g_t^\top$.
 - 7: Update $x_{t+1} = \Pi_{\mathcal{K}}[x_t - \eta G_{t_k}^{-1/2} g_t]$.
 - 8: **end for**
 - 9: **end for**
-

Theorem 18. *Generic Epoch AdaGrad (Alg. 5) with fixed update points $\{t_k\}_{k=1}^K$ satisfies*

$$R_T \leq \frac{D^2}{\eta} \operatorname{tr} G_T^{1/2} + \frac{\eta}{2} \left(2 \operatorname{tr} G_T^{1/2} - 2 \operatorname{tr} G_0^{1/2} + \sum_{k=1}^K \epsilon_k \right),$$

where the error terms ϵ_k are given by

$$\begin{aligned} \epsilon_k &= \operatorname{tr} \left(G_{t_k}^{-1/2} S_k G_{t_k}^{-1/2} A_k \right), \\ S_k &= \int_0^\infty \exp \left(-\tau G_{t_k}^{1/2} \right) A_k \exp \left(-\tau G_{t_k}^{1/2} \right) d\tau, \\ A_k &= G_{t_{k+1}} - G_{t_k}. \end{aligned}$$

Proof of Theorem 18. First we start with the usual decomposition.

Lemma 19. *Consider arbitrary adversarial convex losses f_t . Without projection, the regret R_T relative to a comparator x_* with $D = \max_t \|x_t - x_*\|_2$, for generic epoch AdaGrad with fixed update points t_k is given by*

$$R_T \leq \frac{D^2}{\eta} \operatorname{tr} G_T^{1/2} + \frac{\eta}{2} \sum_{k=1}^K \sum_{t=t_k+1}^{t_{k+1}} g_t^\top G_{t_k}^{-1/2} g_t.$$

Proof of Lemma 19. This follows from the usual AdaGrad analysis since our preconditioners are monotone $G_{t_k} \succeq G_{t_{k+1}}$. \square

So we must turn our attention to the gradient bound. We start by noting the following lemmas established in matrix analysis.

Lemma 20 (Corollary 4.1 in [62]). *The map $f(X) = X^{-1/2}$ is matrix convex over the positive definite domain; i.e., for any two matrices $A, B \succ 0$ and any $\theta \in [0, 1]$, we have*

$$\theta f(A) + (1 - \theta) f(B) \succeq f(\theta A + (1 - \theta) B).$$

Lemma 21 (Theorem V.3.3, Exercise V.3.15 in [63]). *Suppose a matrix convex function $F(X)$ is induced by applying f pointwise to its spectrum $F(X) = U \text{diag}[f(\Lambda_{ii})]U^\dagger$ with $f \in \mathcal{C}^1(I)$ for some $I \subset \mathbb{R}_+$. Then*

$$F(X) + \partial F(X)(\Delta) \preceq F(X + \Delta) ,$$

if and only if $F(X)$ is matrix convex, and the linear transformation $\partial F(X)$ is the derivative of F at X .

Matrix derivative computation [64, 65] shows that if $F(X) = X^{-1/2}$ then

$$\partial F(X)(\Delta) = -X^{-1/2} \left[(X^{1/2} \oplus X^{1/2})^{-1} \Delta \right] X^{-1/2} ,$$

where $(X^{1/2} \oplus X^{1/2})^{-1} \Delta$ is the solution S to the continuous Lyapunov equation $\sqrt{X}S + S\sqrt{X} = \Delta$ as $X \oplus X = I \otimes X + X \otimes I$. For $X \succ 0$, it is known from generic results about Sylvester's equation that the solution S is unique. Since $-X$ is asymptotically stable in the Lyapunov sense,

$$S(X, \Delta) = \int_0^\infty \exp(-\tau\sqrt{X})\Delta \exp(-\tau\sqrt{X}) d\tau .$$

With these results from matrix analysis and linear systems, we are ready to bound the gradient term in Lemma 19. Consider a single term from the gradient bound in Lemma 19, $\sum_{t=t_k+1}^{t_{k+1}} g_t^\top G_{t_k}^{-1/2} g_t$ for fixed k .

With $X = G_{t_k}$, $\Delta = A_k = G_{t_{k+1}} - G_{t_k}$, and $f(X) = X^{-1/2}$ consider applying Lemma 21. $F(X) \preceq F(X + A_k) - \partial F(X)(A_k)$, so overall

$$\begin{aligned} & \sum_{t=t_k+1}^{t_{k+1}} g_t^\top G_{t_k}^{-1/2} g_t \\ & \leq \sum_{t=t_k+1}^{t_{k+1}} g_t^\top \left[G_{t_{k+1}}^{-1/2} - \partial F(G_{t_k})(A_k) \right] g_t \\ & = \sum_{t=t_k+1}^{t_{k+1}} g_t^\top G_{t_{k+1}}^{-1/2} g_t - \text{tr} \left(\partial F(G_{t_k})(A_k) \sum_{t=t_k+1}^{t_{k+1}} g_t g_t^\top \right) \\ & = \sum_{t=t_k+1}^{t_{k+1}} g_t^\top G_{t_{k+1}}^{-1/2} g_t - \text{tr} (\partial F(G_{t_k})(A_k) A_k) \\ & = \sum_{t=t_k+1}^{t_{k+1}} g_t^\top G_{t_{k+1}}^{-1/2} g_t + \text{tr} \left(G_{t_k}^{-1/2} S_k G_{t_k}^{-1/2} A_k \right) \\ & = \sum_{t=t_k+1}^{t_{k+1}} g_t^\top G_{t_{k+1}}^{-1/2} g_t + \epsilon_k . \end{aligned}$$

Lemma 22 (FTL-BTL with errors). *Consider arbitrary ϕ_k for $k \in 0, 1, \dots, K$. Let $x_k \in \text{argmin} \sum_{j=0}^k \phi_j$ and suppose $\phi_k(x_{k-1}) \leq \phi_k(x_k) + \delta_k$. Then $\forall K$,*

$$\sum_{k=0}^K \phi_k(x_{k-1}) \leq \sum_{k=0}^K \phi_k(x_K) + \delta_k ,$$

with $\delta_0 = 0$ and $x_{-1} = x_0$.

Assume Lemma 22 and take $\phi_k(X) = \langle A_k, X \rangle$ for $X \succeq 0$ and $\phi_0(X) = \langle G_0, X \rangle + \text{tr} X^{-1}$. Note that

$$\sum_{j=0}^k \phi_j(X) = \text{tr} X^{-1} + \sum_{j=0}^k \langle A_j, X \rangle .$$

In particular, $G_{t_{k+1}}^{-1/2} = \operatorname{argmin}_{X \succeq 0} \sum_{j=0}^k \phi_j(X)$.

Furthermore, with $\delta_k = \epsilon_k$, the condition $\phi_k(G_{t_k}) \leq \phi_k(G_{t_{k+1}}) + \delta_k$ is satisfied. Lemma 22 implies

$$\begin{aligned} \sum_{k=1}^K \sum_{t=t_k+1}^{t_{k+1}} g_t^\top G_{t_k}^{-1/2} g_t &= \sum_{k=1}^{K-1} \phi_k \left(G_{t_k}^{-1/2} \right) \\ &= -\phi_0(G_0^{-1/2}) + \sum_{k=0}^{K-1} \phi_k \left(G_{t_k}^{-1/2} \right) \\ &\leq -\phi_0(G_0^{-1/2}) + \sum_{k=0}^{K-1} \phi_k \left(G_T^{-1/2} \right) + \epsilon_k , \end{aligned}$$

where $G_{t_0} \stackrel{\text{def}}{=} G_0$. Lastly, since

$$\sum_{k=0}^{K-1} \phi_k \left(G_T^{-1/2} \right) = \operatorname{tr} G_T^{1/2} + \operatorname{tr} \left(G_T^{-1/2} \sum_{k=0}^{K-1} A_k \right) = 2 \operatorname{tr} G_T^{1/2} ,$$

we conclude with the desired bound for R_T . \square

Proof of Lemma 22. By induction on K . For $K = 0$, $\phi_0(x_{-1}) = \phi_0(x_0)$, holding by definition. Suppose that the hypothesis now holds for K ; it then holds for $K + 1$.

$$\begin{aligned} \sum_{k=0}^{K+1} \phi_k(x_{K+1}) &= \sum_{k=0}^K \phi_k(x_{K+1}) + \phi_{K+1}(x_{K+1}) \\ &\geq \phi_{K+1}(x_{K+1}) + \sum_{k=0}^K \phi_k(x_K) \\ &\geq \phi_{K+1}(x_K) - \epsilon_{K+1} + \sum_{k=0}^K \phi_k(x_K) \\ &\geq \phi_{K+1}(x_K) - \epsilon_{K+1} + \sum_{k=0}^K \phi_k(x_{k-1}) - \epsilon_k \\ &\geq \sum_{k=0}^{K+1} \phi_k(x_{k-1}) - \epsilon_k . \end{aligned}$$

\square

G.2 Simplifying the error

We want to simplify the term ϵ_k , which is given by

$$\begin{aligned} \epsilon_k &= \operatorname{tr} \left(G_{t_k}^{-1/2} S_k G_{t_k}^{-1/2} A_k \right) , \\ S_k &= \int_0^\infty \exp \left(-\tau G_{t_k}^{1/2} \right) A_k \exp \left(-\tau G_{t_k}^{1/2} \right) d\tau , \\ A_k &= G_{t_{k+1}} - G_{t_k} . \end{aligned}$$

Next, notice that X and $\exp(-\alpha X^{-1})$ commute. Then along with linearity of trace, we can established that

$$\epsilon_k = \int_0^\infty \operatorname{tr} \left[\left(\exp \left(-\tau G_{t_k}^{1/2} \right) G_{t_k}^{-1/2} A_k \right)^2 \right] d\tau .$$

G.3 Towards simpler error

ϵ_k can be further simplified and bounded under additional assumptions. Namely,

Assumption 1. Suppose that w.p. at least $1 - \delta/2K$ for some fixed, universal $\beta > 0$, we have the inequality $A_k \preceq \beta G_{t_k}$ where $A_k \stackrel{\text{def}}{=} G_{t_{k+1}} - G_{t_k}$.

Assumption 2. Suppose that w.p. at least $1 - \delta/2K$, G_{t_k} 's are $(\sigma_{\min}, \sigma_{\max})$ -well-conditioned, i.e.

$$\lambda_d(G_{t_k}) \geq \sigma_{\min} t_k \quad \text{and} \quad \lambda_1(G_{t_k}) \leq \sigma_{\max} t_k.$$

Remark 23. As an example, consider the stochastic linear setting where at each iteration we receive a loss function $\langle g_t, x \rangle$, and g_t 's are independent, though not necessarily identically distributed, and satisfies that $2\sigma_{\min} I \preceq \mathbb{E}[g_t g_t^\top] \preceq \frac{\sigma_{\max}}{2} I$ and $\|g_t\|_2 \leq \sqrt{\frac{\sigma_{\max}}{2}}$ almost surely. Then, for T sufficiently large and $t_{k+1} - t_k = O(\log T)$, by matrix Chernoff bounds Assumption 1 and 2 are satisfied.

First, $\forall X, Y \succeq 0$, the following inequality hold:

Lemma 24. If $X \preceq Y$ and $A \succeq 0$, then $\text{tr}[(AX)^2] \leq \text{tr}[(AY)^2]$.

With Lemma 24, we can bound ϵ_k . With probability at least $1 - \delta/2K$,

$$\begin{aligned} \epsilon_k &= \int_0^\infty \text{tr} \left[\left(\exp(-\tau G_{t_k}^{1/2}) G_{t_k}^{-1/2} A_k \right)^2 \right] d\tau \\ &\leq \beta^2 \int_0^\infty \text{tr} \left[\left(\exp(-\tau G_{t_k}^{1/2}) G_{t_k}^{-1/2} G_{t_k} \right)^2 \right] d\tau \\ &= \beta^2 \int_0^\infty \text{tr} \left[\left(\exp(-\tau G_{t_k}^{1/2}) G_{t_k}^{1/2} \right)^2 \right] d\tau \\ &= \beta^2 \int_0^\infty \text{tr} \left(\exp(-2\tau G_{t_k}^{1/2}) G_{t_k} \right) d\tau, \end{aligned}$$

where the last step only holds since X and $\exp(-\alpha X^{-1/2})$ commute.

Next, let λ_i denote the i -th largest eigenvalue and λ_{-i} be the i -th smallest. Notice since $\exp(-\tau G_{t_k}^{1/2})$, $G_{t_k}^{1/2}$, and G_{t_k} are simultaneously diagonalizable, and monotonic matrix functions preserve eigenvalue ordering, we have

$$\begin{aligned} \lambda_i \left(\exp(-2\tau G_{t_k}^{1/2}) \right) &= \exp(-2\tau \lambda_{-i} \left((G_{t_k})^{1/2} \right)), \\ \lambda_i \left(\exp(-2\tau G_{t_k}^{1/2}) G_{t_k} \right) &= \lambda_i \left(\exp(-2\tau G_{t_k}^{1/2}) \right) \lambda_i(G_{t_k}). \end{aligned}$$

Returning to our ϵ_k bound, rewriting the trace with eigenvalues, we have w.p. at least $1 - \delta/2K$,

$$\begin{aligned} \epsilon_k &\leq \beta^2 \int_0^\infty \sum_i \lambda_i \left(\exp(-2\tau G_{t_k}^{1/2}) G_{t_k} \right) d\tau \\ &= \beta^2 \sum_i \lambda_i(G_{t_k}) \int_0^\infty \exp(-2\tau \lambda_{-i}(G_{t_k})^{1/2}) d\tau \\ &= \beta^2 \sum_i \frac{\lambda_i(G_{t_k})}{2\lambda_{-i}(G_{t_k})^{1/2}}, \end{aligned}$$

where \leq_1 follows from Tonelli's Theorem. At this point, we apply Assumption 2 and get that w.p. at least $1 - \delta/K$,

$$\begin{aligned}
\epsilon_k &\leq \frac{\beta^2}{\sqrt{t_k \sigma_{\min}}} \sum_i \lambda_i(G_{t_k}) \\
&\leq \frac{\beta^2}{\sqrt{t_k \sigma_{\min}}} \sum_i (t_k \sigma_{\max})^{1/2} \lambda_i(G_{t_k})^{1/2} \\
&= \beta^2 \sqrt{\frac{\sigma_{\max}}{\sigma_{\min}}} \sum_i \lambda_i(G_{t_k})^{1/2} \\
&= \beta^2 \sqrt{\frac{\sigma_{\max}}{\sigma_{\min}}} \text{tr} G_{t_k}^{1/2}.
\end{aligned}$$

Across all epochs, we then have w.p. at least $1 - \delta$,

$$\frac{1}{\beta^2} \sqrt{\frac{\sigma_{\min}}{\sigma_{\max}}} \sum_{k=1}^K \epsilon_k \leq \sum_{k=1}^K \text{tr} G_{t_k}^{1/2} \leq \log T \text{tr} G_T^{1/2}.$$

Altogether, since β is a universal constant, w.p. at least $1 - \delta$,

$$R_T \lesssim \frac{D^2}{\eta} \text{tr} G_T^{1/2} + \eta \sqrt{\frac{\sigma_{\max}}{\sigma_{\min}}} \log T \text{tr} G_T^{1/2}.$$

We conclude that in this case, the time dependency of Epoch AdaGrad's regret is only $\log T$ factor worse than that of the original AdaGrad regret.

G.3.1 Proof of Lemma 24

First, for $0 \preceq X \preceq Y$, $BXB \preceq BYB$, $\forall B$, since $(Bx)^\top (Y - X)(Bx) \geq 0$, $\forall x$. By cyclic property of trace and taking $B = A^{1/2}X$,

$$\text{tr}(AXAX) = \text{tr}\left(X^{1/2}AXAX^{1/2}\right) \leq \text{tr}\left(X^{1/2}AYAX^{1/2}\right).$$

Continuing,

$$\begin{aligned}
\text{tr}\left[(AX)^2\right] &\leq \text{tr}\left(X^{1/2}AYAX^{1/2}\right) \\
&= \text{tr}\left(Y^{1/2}AXAY^{1/2}\right) \\
&\leq \text{tr}\left(Y^{1/2}AYAY^{1/2}\right) \\
&= \text{tr}\left[(AY)^2\right].
\end{aligned}$$